HIROSHIMA MATH. J.
37 (2007), 343–384

A billiard problem in nonlinear and nonequilibrium systems

Masayasu MIMURA, Tomoyuki MIYAJI and Isamu OHNISHI

(Received December 22, 2005)
(Revised July 11, 2006)

ABSTRACT. In this paper a billiard problem in nonlinear and nonequilibrium systems is investigated. This is an interesting problem where a traveling pulse solution behaves as if it is a billiard ball at a glance in some kind of reaction-diffusion system in a rectangular domain. We would like to elucidate the characteristic properties of the solution of this system. For the purpose, as the first step, we try to make a reduced model of discrete dynamical system having the important properties which the original system must have. In this paper we present a discrete toy model, which is reduced intuitively as one of the candidates by use of numerical experiments and careful observation of the solutions. Moreover, we discuss about the similar and important points between the solution in the original ordinary differential equation (which describes the pulse behavior) and the one in the toy model by computing numerically the characteristic quantities in view of the dynamical system, for example, global and local Lyapunov exponents and Lyapunov dimensions. As a result, we elucidate that the system possesses an intermittent-type chaotic attractor.

1. Introduction

In a certain class of reaction-diffusion system in which its stationary pulse solution loses its stability and a traveling pulse solution arises, as a parameter changes, if this solution is confined in a rectangular domain, then this solution moves as if it is a billiard ball at a glance. The self-motion of the camphor disk is an example of such systems. Let us make the following experiment: The camphor disk is made of the condensation of camphor and impurities-(cornstarch). Pour water into the water tank and then float the camphor disk on the surface of the water. Then the difference of the surface tension arises from the dissolution of camphor to water. If the purity of camphor is higher than the critical value, then the camphor disk is pulled to the surface tension low and moves like a billiard ball repeating the uniform motion and the

The second author is supported by a grant of "Initiative program of facinating educations of graduate school" in Ministry of Education, Culture, Sports, Science and Technology in Japan. The last author is supported by Grant No. 15540122 and No. 17540118 of JSPS.

2000 *Mathematics Subject Classification.* 37M05, 37M20, 37M25, 37N30.

Key words and phrases. nonlinear and nonequilibrium system, billiard problem, reduction to the discrete-time system, Lyapunov exponents and Lyapunov dimension.

reflection. But this system is quite different from the usual billiard problem in the point of view of revenue and expenditure of kinetic energy. Unlike the usual billiard problem with the energy conservation law, there is expenditure of kinetic energy by friction and is revenue by its solving. In a word, it can be said that this is a good example of non-equilibrium and nonlinear phenomena.

We can reduce the reaction-diffusion system with such a pulse solution to the particle model, which is regarded as a singular limit equation as the pulse size tends to zero. Derivation of the particle model is described in detail in [1]. As we make a numerical simulation of the particle model, at a glance, the solution seems also to behave similarly to the usual billiard problem. But if we investigate the behavior of the solution in details, then we notice that the solution behaves with more complex motion than in the usual billiard problem even in a rectangular domain. In fact, we can see a various of behavior of the solution as the aspect ratio of the rectangular domain changes. Especially in some parameter intervals, the solution behaves even chaotically, which can not be seen in the usual problem in rectangular domain. We would like to know what makes such a kind of differences between them.

In this paper, we study this interesting problem by mainly use of numerical simulations. In §2, we make a research of the solution of the particle model in details. We first investigate the relationship of the angle of incidence and of reflection, in which we can find the primitive difference of the usual billiard problem. Next, we draw a kind of bifurcation diagram of orbits of the problem, in which we can see chaotic parameter regions exist intermittently. These results have been already reported in [4], [5], and [6]. But, as those are written in Japanese, we report again them here to make sure of them, too. Moreover, we compute Lyapunov exponents and Lyapunov dimensions for some interesting parameters and verify that the strange solutions have chaotic property by numerical simulations.

In §3, we investigate what is the mechanism of the strange behavior of the system under consideration. For the purpose, we reduce the system of equations to a discrete-time dynamical system model. As it is very hard to reduce the system theoretically to the discrete one, we do it with intuitive way by use of numerical simulation to get a kind of toy model. We first make observations of the solutions of the particle model, and get a characteristic property of the solution of the system. Especially, we pay attention to a strange behavior of the solution near the corners of the rectangle. Next, we present a toy model of the modified discrete-time model as a candidate which has the desirable properties of strange behavior of the solution especially near corners.

Finally we make investigations about this toy model to see this model possess the very similar properties to the particle model in view of dynamical

system. Especially this model has the intermittent chaotic behavior of the solution. Therefore we expect that the strange behavior of the solution which we found near corners is essential to the interesting behavior of the system under consideration. We make a conclusion that this strange behavior of the solution is due to existence of the intermittent-type chaotic attractor in the system.

2. Particle model

2.1. Mathematical models which describe the motion of camphor disks. To understand the self-motion of camphor disks theoretically, some mathematical models have been introduced. The main models are as follows:

(1) Point mass approximation model [3]
(2) Moving-boundary model
(3) Particle model.

Here we treat the particle model which is derived as a reduction system of the moving-boundary model under the assumption that the speed where the camphor disk moves is very slow. First of all, we introduce it.

The moving-boundary model is described as follows: Let $u(t,x)$ be the concentration of dissolved camphor. And d is diffusion rate of dissolved camphor, μ is a viscosity, k is the sum of sublimation rate and dissolution rate, and α is a dissolution rate of solid camphor. The surface tension is represented by

$$\gamma(u) = \frac{\gamma_0}{cu+1},$$

where γ_0 is the surface tension of water and c is a positive constant. The model equation is described as

$$\begin{cases} u_t = d\Delta u - ku + \begin{cases} \alpha & t>0,\ x\in\Omega(t), \\ 0 & t>0,\ x\in S\backslash\Omega(t), \end{cases} \\ \mu V = c\int_{\partial\Omega(t)} \gamma(u)d\vec{s} \quad t>0,\ x\in\partial\Omega(t), \end{cases}$$

where $\Omega(t)$ is the disk domain of radius r corresponding to a camphor disk, S is the domain corresponding to a water tank, and V is the velocity of the center of a camphor disk. This can be reduced to an ordinary differential equations under the assumption that the speed where the camphor disk moves is very slow. See [1] about details. The motion of camphor disk in two dimensional plane $\mathbf{R}^2$ is described by its center coordinate and velocity. Let $P(t) = (x(t), y(t))$ and $V(t) = (v(t), w(t))$ be its center coordinate and velocity respectively, then we can consider a camphor disk as one point particle. Now

particle model is described by the following four dimensional ordinary differential equations:

$$\begin{cases} \dot{x} = v, \\ \dot{y} = w, \\ \dot{v} = -(m_1|V|^2 v + m_2 \varepsilon v), \\ \dot{w} = -(m_1|V|^2 w + m_2 \varepsilon w), \end{cases} \tag{1}$$

where $|V|^2 = v^2 + w^2$ and m_1, m_2 are positive constants and ε is a parameter corresponding to the purity of camphor.

The system (1) is analyzed in [5]. The motion of a particle described by (1) has following properties: In the case $\varepsilon > 0$, the moving particle will stop before long for any initial velocity. On the other hand, in the case $\varepsilon < 0$, if $|V(0)| = 0$, then any $t > 0$ the particle won't leave an initial position. If $|V(0)| \neq 0$, then the motion of a particle will converge asymptotically to uniform motion.

Secondly, we consider the motion of two particles which have the interaction. Let $P_I(t) = (x_I(t), y_I(t))$ and $V_I(t) = (v_I(t), w_I(t))$ $(I = 1, 2)$ be their coordinate and velocity. Then the motion of these two particles is described by following eight dimensional ordinary differential equations:

$$\begin{cases} \dot{x}_I = v_I - m_0 h^{-3/2} \exp(-ah)(x_{I+1} - x_I), \\ \dot{y}_I = w_I - m_0 h^{-3/2} \exp(-ah)(y_{I+1} - y_I), \\ \dot{v}_I = -(m_1|V_I|^2 v_I + m_2 \varepsilon v_I) - m_3 h^{-3/2} \exp(-ah)(x_{I+1} - x_I), \\ \dot{w}_I = -(m_1|V_I|^2 w_I + m_2 \varepsilon w_I) - m_3 h^{-3/2} \exp(-ah)(y_{I+1} - y_I), \end{cases} \tag{2}$$

where we agree to interpret I modulo 2, $h = |P_1 - P_2|$ is the distance between two particles and m_j $(j = 0, 1, 2, 3)$ and a are positive constants. If $h \gg 1$, that is, the distance between two particles is sufficiently large, then the interaction term $h^{-3/2} \exp(-ah)$ becomes very small. Hence we can consider that $(P_1(t), V_1(t))$ and $(P_2(t), V_2(t))$ are independent with each other in that case.

Next, we consider the motion of a particle that approaches the wall. In this case, let y-axis be the reflecting wall. We assume that there is another virtual particle at a symmetrical position for the wall and consider the interaction between these particles by using 2. Let $P_1(t_0) = (x_0, y_0)$ and $V_1(t_0) = (v_0, w_0)$ be the initial position and velocity of a particle. Then according to symmetry, the initial condition of virtual particle is $P_2(t_0) = (-x_0, y_0)$ and $V_2(t_0) = (-v_0, w_0)$. Following [5], $(P_1(t), V_1(t))$ and $(P_2(t), V_2(t))$ are always located at a symmetrical position for any $t > 0$. Therefore we can rewrite 2 by introducing new variables $(x, y, v, w) = (x_1, y_1, v_1, w_1)$ as follows:

$$\begin{cases} \dot{x} = v + m_0(2x)^{-1/2}\exp(-2ax), \\ \dot{y} = w, \\ \dot{v} = -(m_1|V|^2 v + m_2\varepsilon v) + m_3(2x)^{-1/2}\exp(-2ax), \\ \dot{w} = -(m_1|V|^2 w + m_2\varepsilon w). \end{cases} \tag{3}$$

Notice that (3) is essentially a three dimensional system since x, v and w are independent of y.

Finally, as an extension of (3), we introduce the model which describes the motion in a rectangular domain $R = [0, cL] \times [0, L]$. In this case, we assume that there are four virtual particles at a symmetrical position for each edge of R and consider the interaction between five particles. As well as the previous case, by using symmetry, we get the particle model in a rectangular domain as follows:

$$\begin{cases} \dot{x} = v + m_0\dfrac{\exp(-2ax)}{\sqrt{2x}} - m_0\dfrac{\exp(-2a(cL-x))}{\sqrt{2(cL-x)}}, \\ \dot{y} = w + m_0\dfrac{\exp(-2ay)}{\sqrt{2y}} - m_0\dfrac{\exp(-2a(L-y))}{\sqrt{2(L-y)}}, \\ \dot{v} = -(m_1|V|^2 v + m_2\varepsilon v) + m_3\dfrac{\exp(-2ax)}{\sqrt{2x}} - m_3\dfrac{\exp(-2a(cL-x))}{\sqrt{2(cL-x)}}, \\ \dot{w} = -(m_1|V|^2 w + m_2\varepsilon w) + m_3\dfrac{\exp(-2ay)}{\sqrt{2y}} - m_3\dfrac{\exp(-2a(L-y))}{\sqrt{2(L-y)}}. \end{cases} \tag{4}$$

2.2. Numerical simulations. When the camphor disk floats on water, it moves almost in uniform motion if away from the wall. And if it approaches the wall, it reflects without collision with a wall. Furthermore, this reflection has the property that the angle of reflection is smaller than that of incidence. We confirm that the solutions of (3) show such a reflection by numerical simulation.

We set parameters $m_i = 1.0$ $(i = 0, 1, 2, 3)$, $a = 1.0$, $\varepsilon = -0.06$. Then we can see that the particle reflects without collision with a wall (See Figure 1).

Next, we observe the relation between angles of incidence and reflection. But we can't define angle near the wall since the particle reflects while drawing a curve without collision with a wall as shown in Figure 1. So we use the property that particles move almost in uniform motion if it sufficiently away from the wall. Let (v_0, w_0) be the initial velocity which is given at the initial position where sufficiently away from wall and (v_∞, w_∞) be the velocity in state

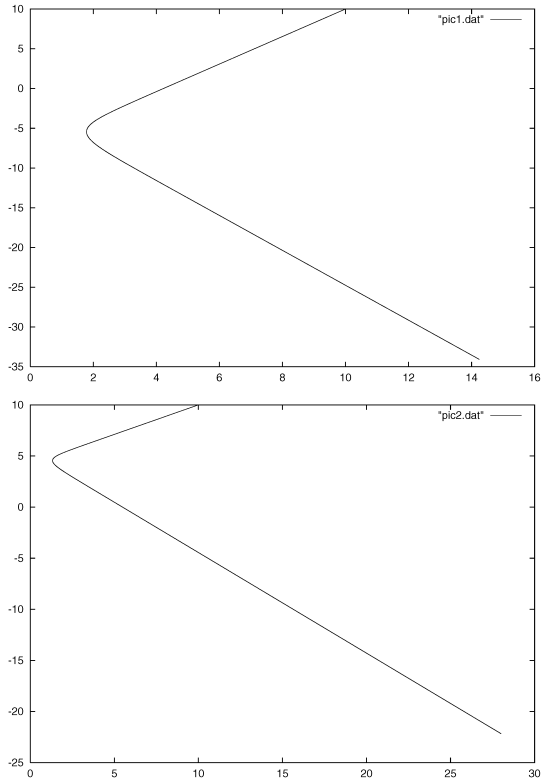

Fig. 1. Reflection near the wall (Projection onto (x, y)-plane).

of uniform motion after reflection. Then we define the angle of incidence θ_{in} and the angle of reflection θ_{out} by

$$\theta_{\text{in}} = \arctan\left(\frac{v_0}{w_0}\right), \qquad \theta_{\text{out}} = \arctan\left(\frac{v_\infty}{w_\infty}\right).$$

Figure 2 is the relation between θ_{in} and θ_{out}, $\theta_{\text{out}} = F(\theta_{\text{in}})$, obtained by numerical experiments. As shown in figure, this reflection is not perfect elastic reflection but non-perfect elastic reflection and $\theta_{\text{in}} > \theta_{\text{out}}$ for $\theta_{\text{out}} \in (0, \pi/2)$.

Then, we simulate the system (4), the particle in a rectangular domain $R = [0, cL] \times [0, L]$. First, let the aspect ratio of the domain c be $c = 1.0$, that is, we consider the case where R is a square. We set parameters $m_i = 1.0$ $(i = 0, 1, 2, 3)$, $a = 1.0$, $\varepsilon = -0.06$ and $L = 20.0$. Assume that the initial condition is $(x_0, y_0) = (10.0, 10.0)$, $(v_0, w_0) = (\sqrt{-\varepsilon}\sin\theta, -\sqrt{-\varepsilon}\cos\theta)$, then the asymptotic orbit can be qualitatively classified into three kinds for the value of θ. See Figure 3.

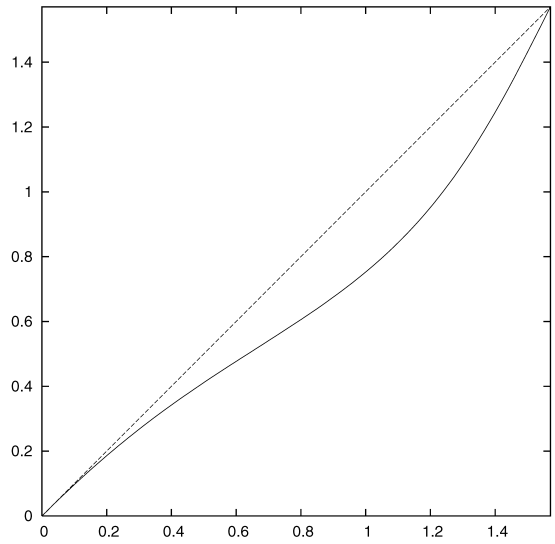

Fig. 2. Relation between θ_{in} and θ_{out} $(\varepsilon = -0.06)$.

About quadrangle orbit shown in Figure 3, as shown in Figure 4, there is a reverse-rotation orbit in the domain. Though two orbits in Figure 4 are different the direction of the rotation, these are corresponding by reversing. It is suggested by numerical simulation that the orbit of (4) in a square domain converges to a certain periodic orbit for any initial condition and orbits shown in Figure 4 are asymptotically stable periodic orbit.

Next, we consider how the orbit changes when the domain is changed from the square into the rectangle. Change the aspect ratio c in (4) and solve the system numerically.

If the parameter c is near 1.0, for almost every initial value the orbit converges to a certain periodic orbit as shown in Figure 5. As c grows, the round-cornered rectangle drawn by the stable periodic orbit becomes thin. However, c grows greater than a certain value, solutions of (4) draw complex orbits shown in Figure 6.

To know the relation between c and the asymptotic orbit at this parameter value better, we introduce the following diagrams: Assign the parameter c to the horizontal axis and the reflection position at the wall $y = 0$ to the vertical axis. However, since it is difficult to specify coordinates that the velocity in the vertical direction becomes zero, x-coordinates where the absolute value of the velocity in the vertical direction becomes sufficiently small are recorded. And the x-coordinates are divided by c so that the value is between zero and L. The resulting picture is Figure 7. It was confirmed that depending on the

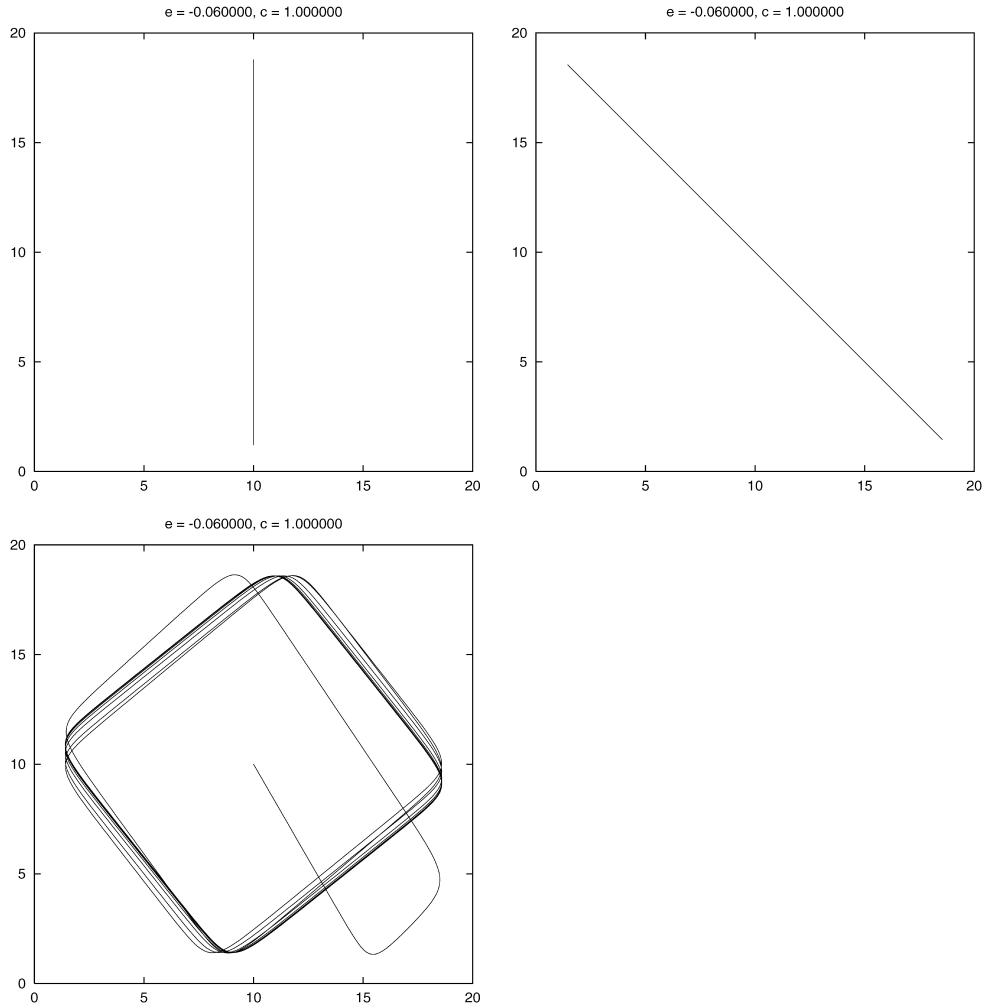

Fig. 3. Three kinds of orbits in square.

value of the parameter c the motion of the particle alternately repeated the periodic orbit and non-periodic orbit. It seems that typical intermittent chaos appears. Figure 8 is a set of some periodic orbits in Figure 7. For large c, such complex periodic orbits appear.

2.3. Calculation of Lyapunov exponents. We consider whether non-periodic orbits in the particle model (4) are chaos. So we calculate Lyapunov exponents and quantify the stability of the orbit on the attractor. The numerical calculation method of Lyapunov exponents is detailed in the references [8], [7], and

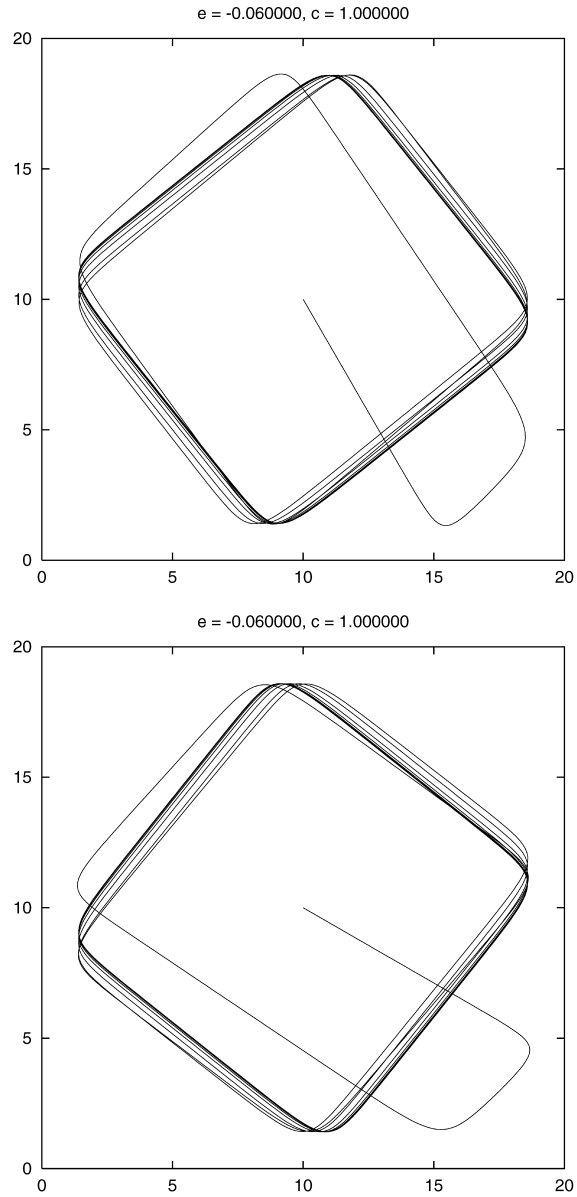

Fig. 4. Quadrangle periodic orbit in square.

[2]. We calculated exponents for several c from 1.0 to 5.0. The calculation result is as follows: For simple periodic orbits that appear near $c = 1.0$, the sign of Lyapunov exponents is $(0, -, -, -)$ and Lyapunov dimension d_{L} is equal to 1.0. And for periodic orbits at large c, the result is the same. For

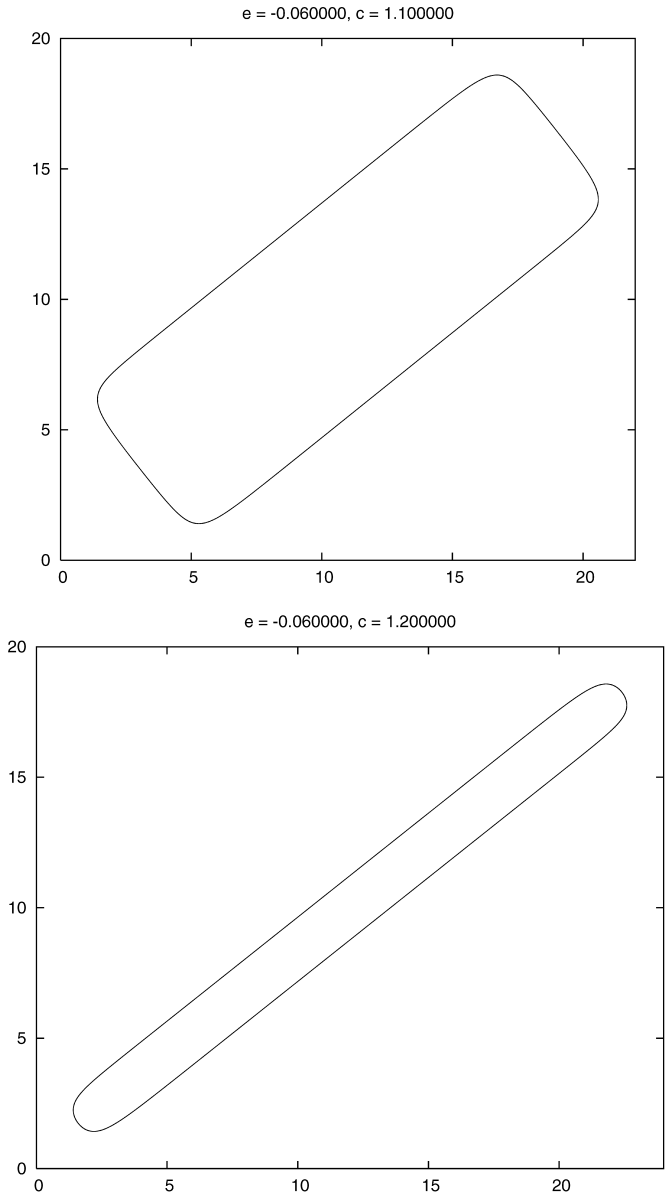

Fig. 5. Stable periodic orbits at $c = 1.1$ (left) and $c = 1.2$ (right).

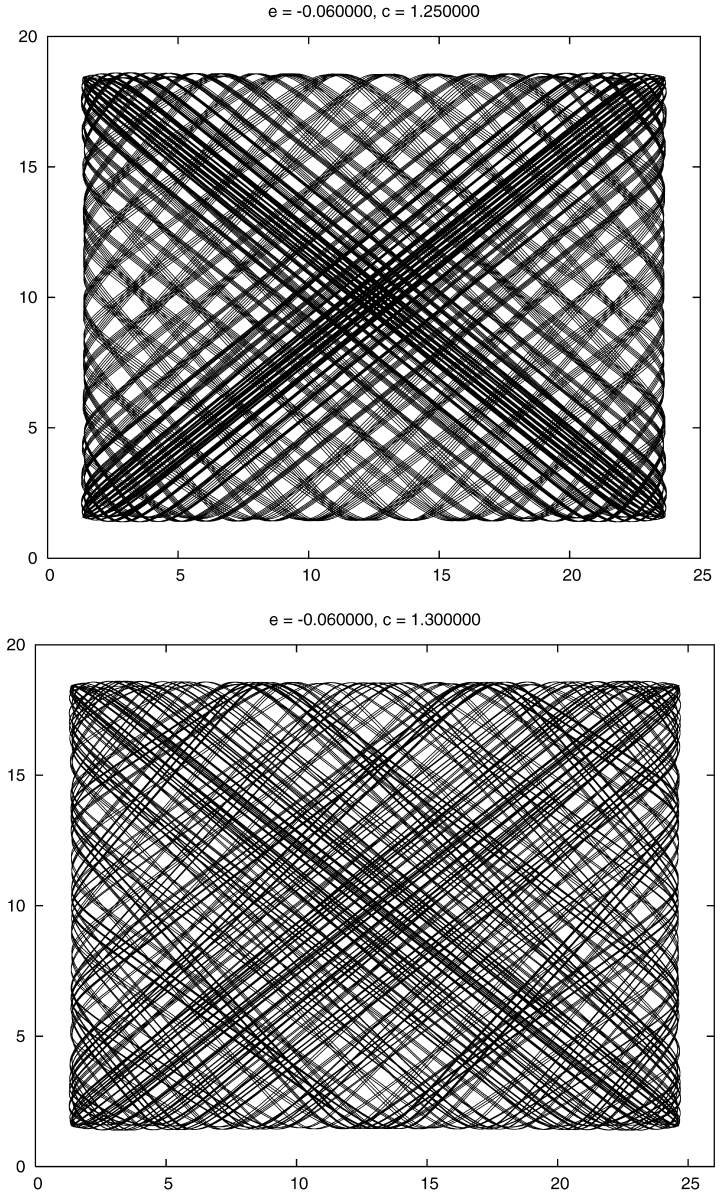

Fig. 6. Complex orbits at $c = 1.25$ (left) and $c = 1.3$ (right).

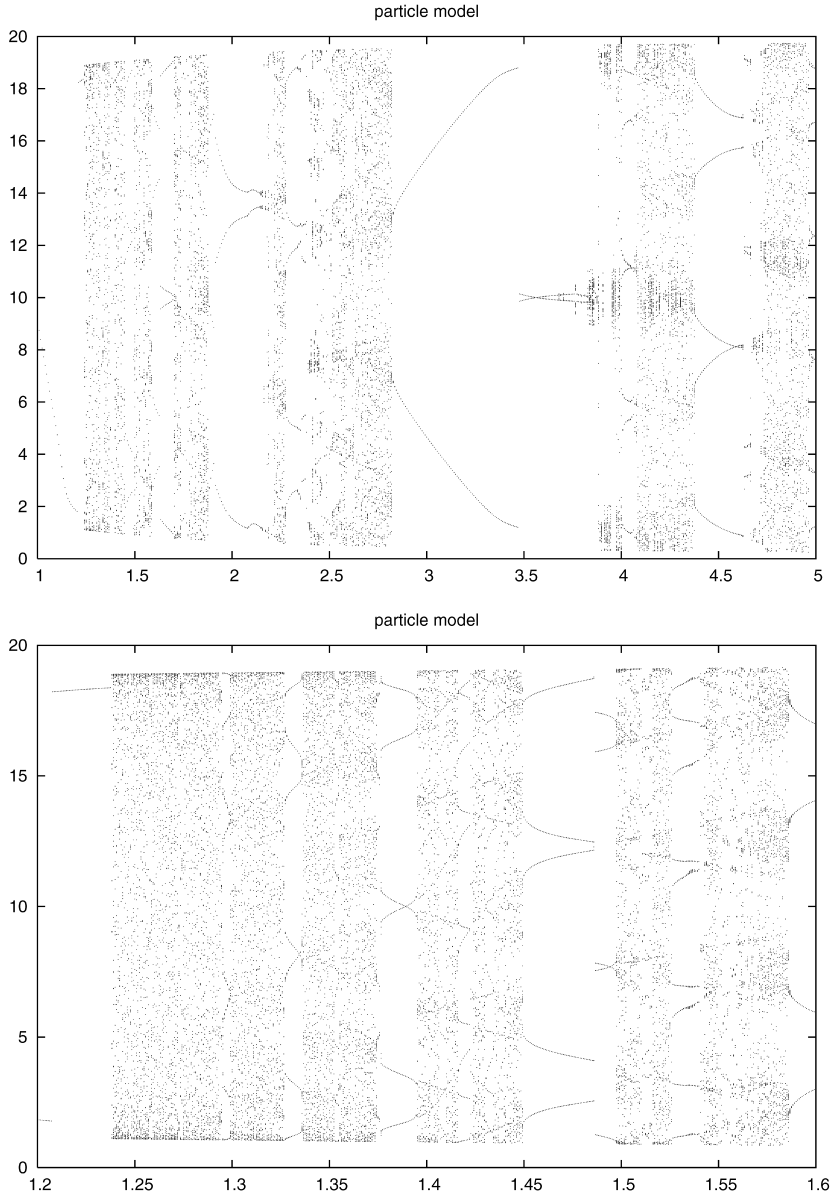

Fig. 7. Relation between the parameter c and reflection positions (left: $1.0 < c < 5.0$, right: $1.2 < c < 1.6$).

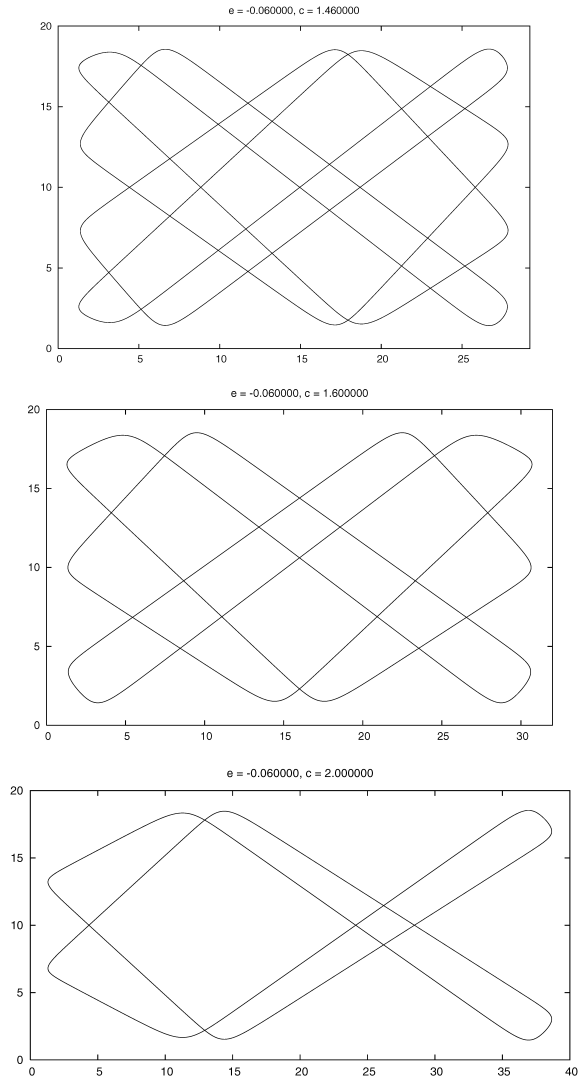

Fig. 8. Periodic orbits for several parameters $(c = 1.46, 1.6, 2.0, 2.9, 4.4)$.

the orbit seen to be non-periodic at $c = 1.3$, the sigh of exponents is $(0, 0, -, -)$ and $d_{\mathrm{L}} = 2.0$. Thus though this orbit fills the domain, this might not be chaotic. However, for other parameters, a positive exponent might be obtained. In this case, the sign of exponents is $(+, 0, -, -)$ and $2 < d_{\mathrm{L}} < 3$. Hence it can be expected that these orbits are chaotic.

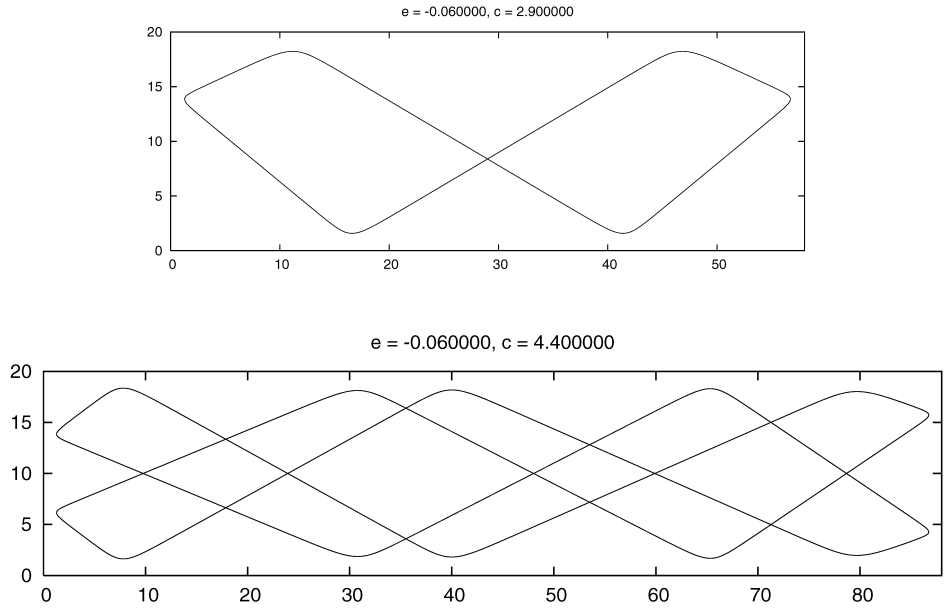

Fig. 8. Continued

Table 1. Lyapunov exponents and dimension for several c.

Parameter values	Lyapunov spectrum	Lyapunov dimension
$c = 1.00$	$\lambda_1 = 0.0000,\ \lambda_2 = -0.0057$	1.0000
	$\lambda_3 = -0.0093,\ \lambda_4 = -0.1600$	
$c = 1.30$	$\lambda_1 = 0.0000,\ \lambda_2 = 0.0000$	2.0000
	$\lambda_3 = -0.0102,\ \lambda_4 = -0.1587$	
$c = 1.40$	$\lambda_1 = 0.0000,\ \lambda_2 = -0.0006$	1.0000
	$\lambda_3 = -0.0095,\ \lambda_4 = -0.1593$	
$c = 1.85$	$\lambda_1 = 0.0007,\ \lambda_2 = 0.0000$	2.0680
	$\lambda_3 = -0.0099,\ \lambda_4 = -0.1617$	
$c = 2.24$	$\lambda_1 = 0.0015,\ \lambda_2 = 0.0000$	2.1687
	$\lambda_3 = -0.0090,\ \lambda_4 = -0.1633$	
$c = 2.82$	$\lambda_1 = 0.0003,\ \lambda_2 = 0.0000$	2.0364
	$\lambda_3 = -0.0076,\ \lambda_4 = -0.1649$	
$c = 3.00$	$\lambda_1 = 0.0000,\ \lambda_2 = -0.0029$	1.0000
	$\lambda_3 = -0.0042,\ \lambda_4 = -0.1652$	
$c = 3.99$	$\lambda_1 = 0.0021,\ \lambda_2 = 0.0000$	2.3703
	$\lambda_3 = -0.0057,\ \lambda_4 = -0.1675$	
$c = 4.88$	$\lambda_1 = 0.0013,\ \lambda_2 = 0.0000$	2.2510
	$\lambda_3 = -0.0052,\ \lambda_4 = -0.1682$	

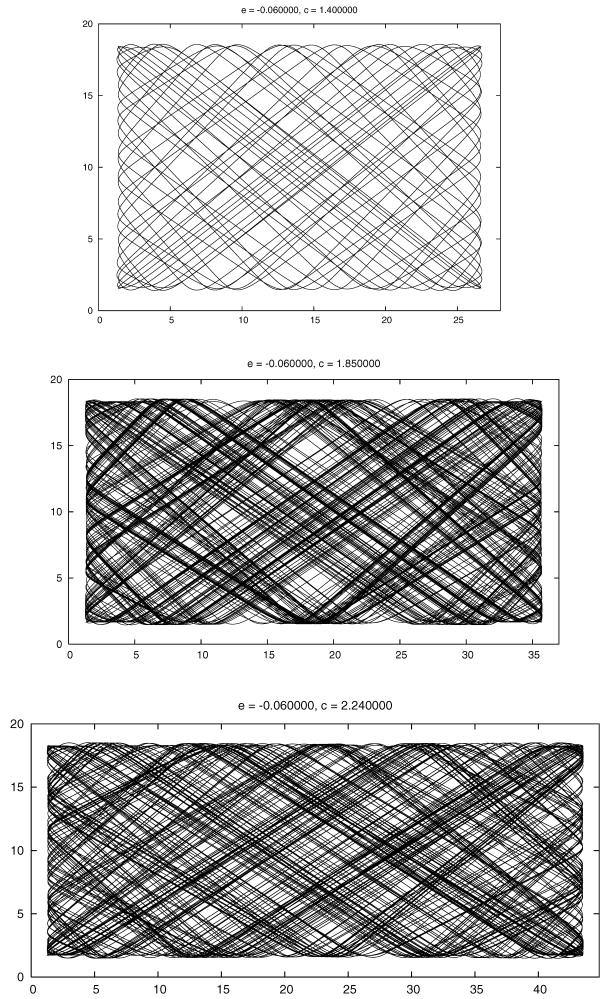

Fig. 9. Non-periodic orbits for $c = 1.40, 1.85, 2.24, 2.82, 3.99, 4.88$.

3. Discrete-time model

3.1. Derivation of discrete-time model. The particle model is derived as a reduction system of a certain reaction-diffusion system near the bifurcation point at which a stationary pulse solution of the system loses stability and a traveling pulse solution arises. However, this model is still too complex to analyze it. We are interested in the global bifurcation structure of the solution of this system that intermittent chaos seems to appear. So we describe orbits of the particle model as a discrete-time dynamical system with lower dimension

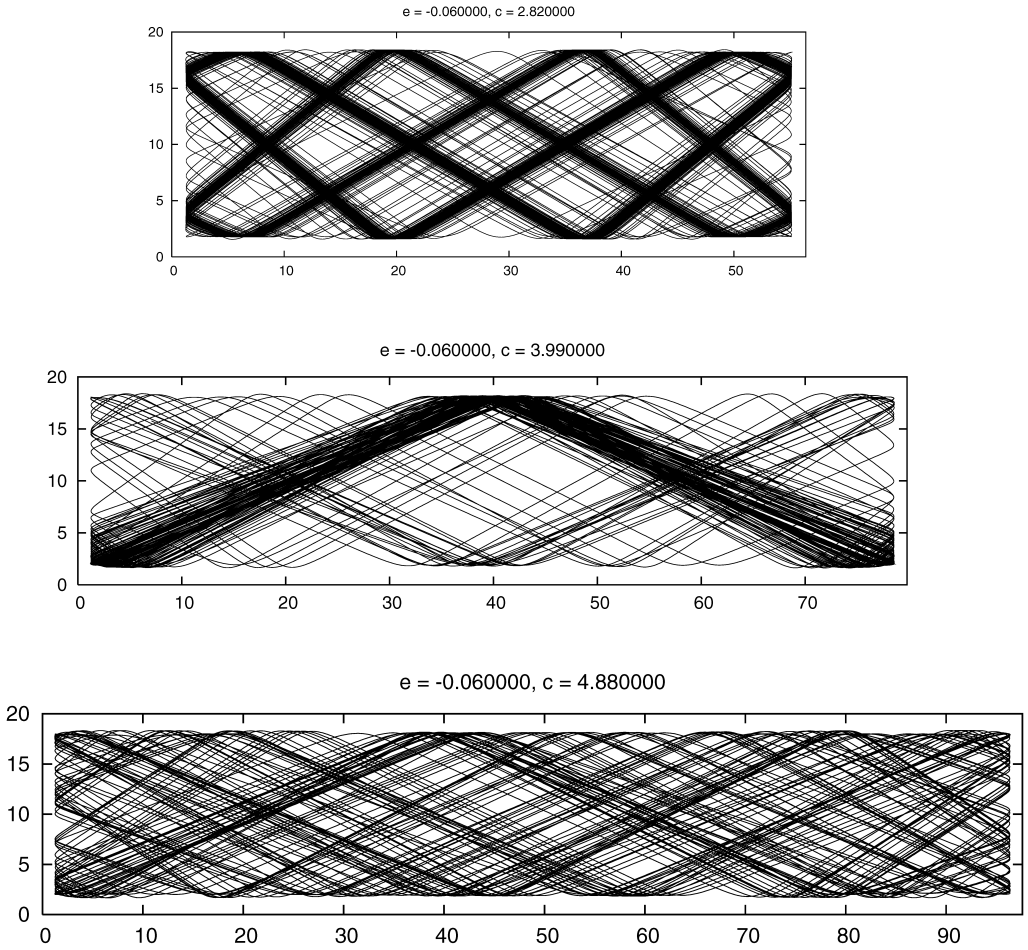

Fig. 9. Continued

by using a limit operation proposed in [4] and [6]. We execute the following limit operation: Assume that $L = \infty$ and consider reflection of the orbit of the particle model. Shorten the length of a edge of the square domain L again.

By such an operation, we can consider that the particle is in a state of uniform motion in the square domain and hits the wall and reflects. And θ_{in} and θ_{out} are given by the relation $\theta_{\text{out}} = F(\theta_{\text{in}})$ shown in Figure 2.

It is easy to prove the existence and uniqueness of a stable periodic orbit in the square for this discrete-time model. It is discussed in detail in [4] and [6].

Then, we consider the case in a rectangular domain. Indeed, it is possible to prove the unique existence of a stable periodic orbit in a rectangular domain

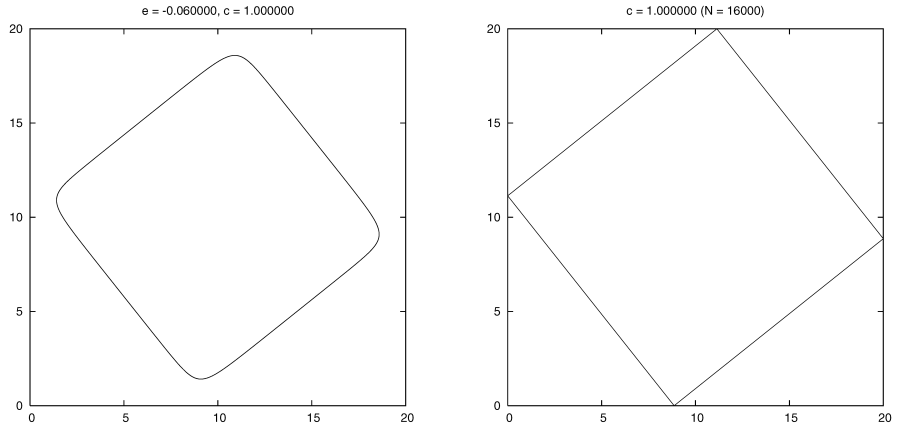

Fig. 10. Stable periodic orbit in the square domain (left: particle model, right: discrete-time model).

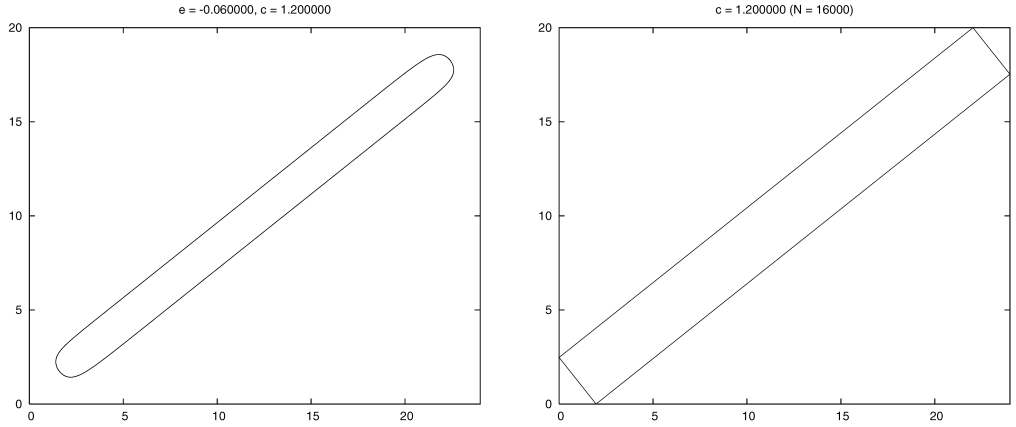

Fig. 11. Stable periodic orbit for $c = 1.2$ (left: the particle model, right: the discrete model).

by using of this discrete-time model. It is discussed in detail in [4], [6]. See Figures 11 and 12. This discrete-time model reproduces the stable periodic orbit well in particle model.

However, this attempt fails in the approximation of non-periodic orbit. Figure 13 is a comparison of the particle model and the discrete-time model for $c = 1.3$. The particle model shows non-periodic orbit for $c = 1.3$. On the other hand, an asymptotic orbit in the discrete-time model for $c = 1.3$ is not non-periodic though it is complex. We compare the dependency of asymptotic orbits on c for the particle model with that for the discrete model. See Figure 14. It shows the relation between c and reflection positions at the wall $y = 0$.

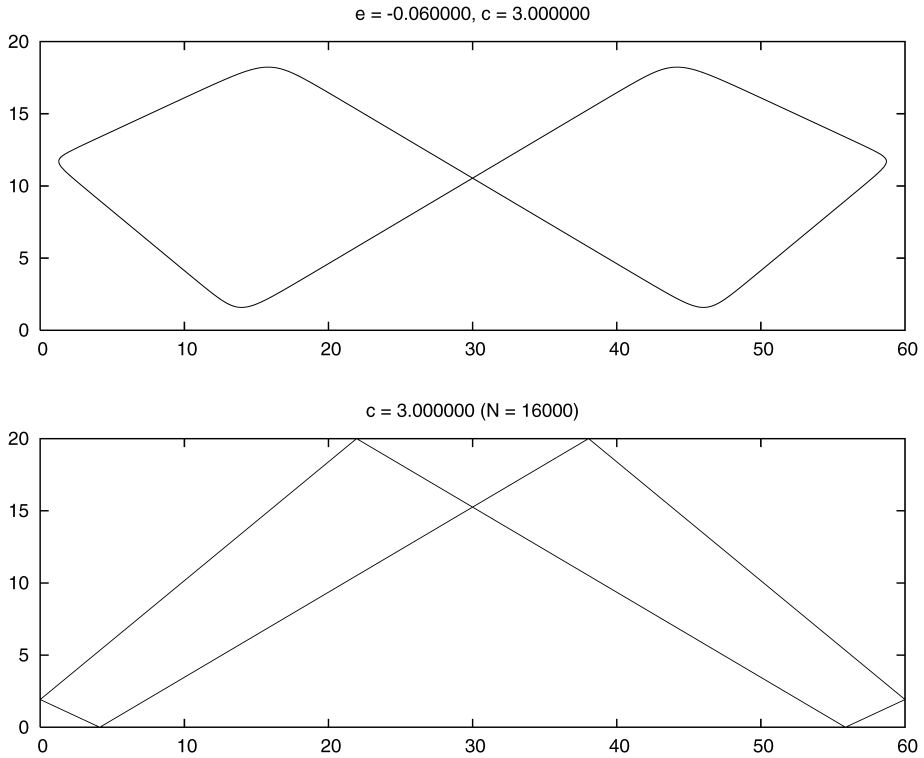

Fig. 12. Stable periodic orbit for $c = 3.0$ (upper: the particle model, lower: the discrete model).

For the discrete-time model, there seems to be no non-periodic structure. This discrete-time model cannot be applied to the analysis of non-periodic orbit.

3.2. Observe the particle model. Why does such a difference appear between the discrete-time model and the particle model? We compare a greatly different point in two models and enable the application to non-periodic orbit by adding a proper correction to the discrete model.

The most remarkable difference is pointed out by [6]. When the particle reflects near the center of the wall, the orbit of the discrete-time model coincides with that of the particle model. However, when the particle reflects near the corner of the domain, these orbits do not coincide. In this case, the particle starts the next reflection before it turn into a state of uniform motion after the reflection first. Thus the angle of incidence of the second reflection is different in both models. Two orbits of the particle model toward the same direction starting from different initial positions is shown in Figure 15.

Though it is incidence at the same angle, the angle of reflection is different.

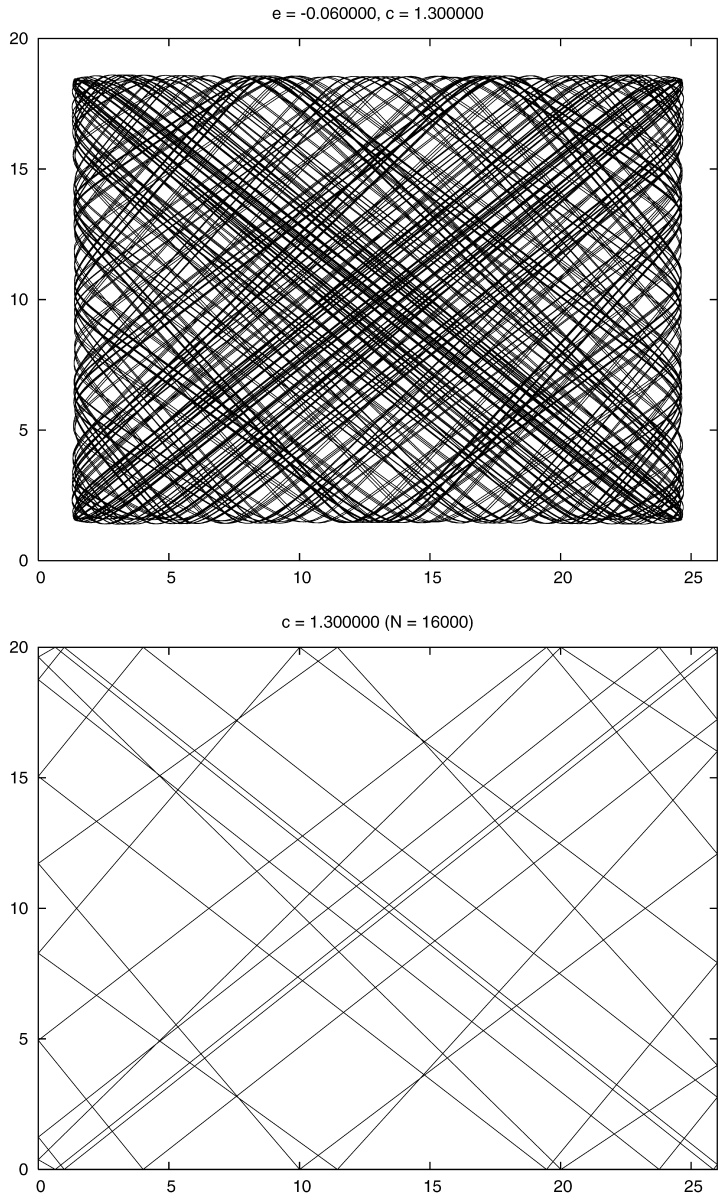

Fig. 13. Asymptotic orbit for $c = 1.3$ (upper: the particle model, lower: the discrete model).

It is thought that this is because the interaction with the wall changes by the reflection position. When non-periodic orbit appears, the particle fills the area by repeating the reflection near the corner. To observe the influence of the reflection in the corner, we calculate local Lyapunov exponents.

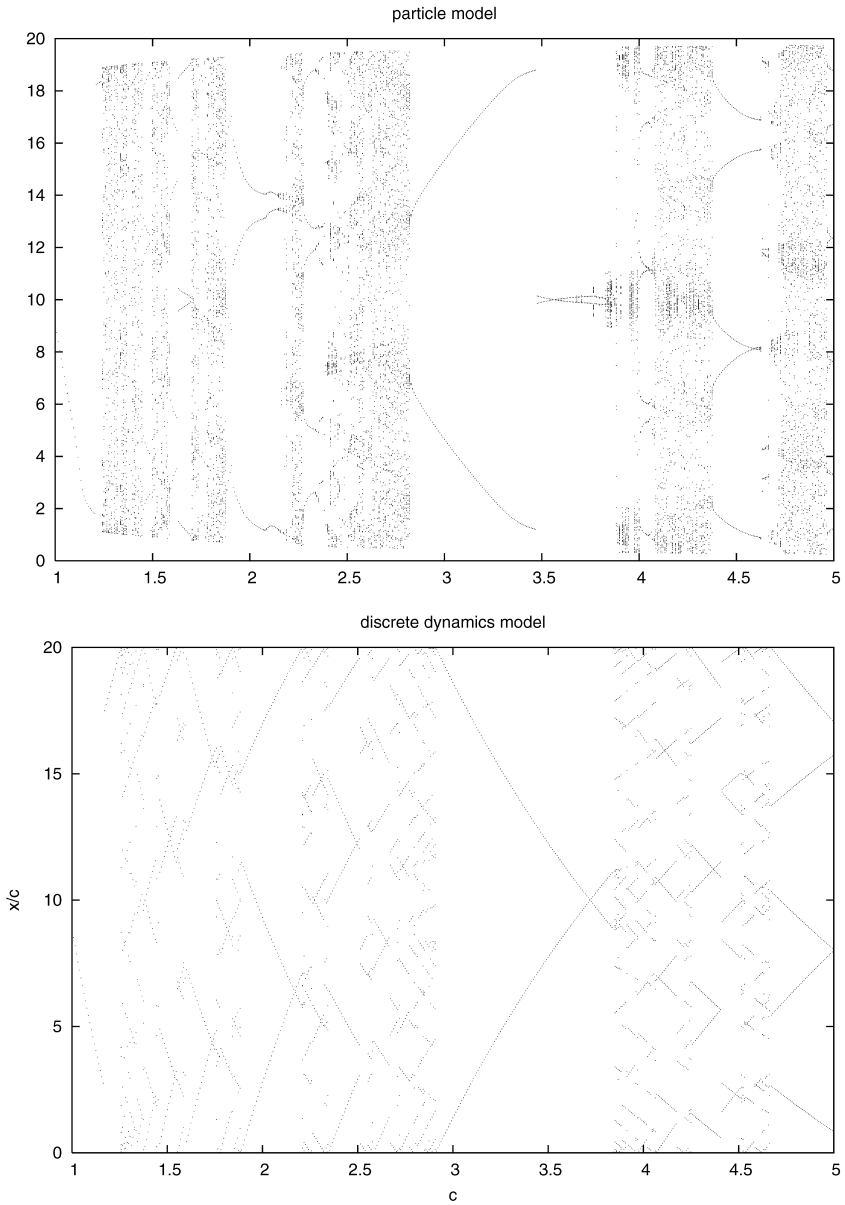

Fig. 14. The relation between c and reflection positions (upper: the particle model, lower: the discrete model).

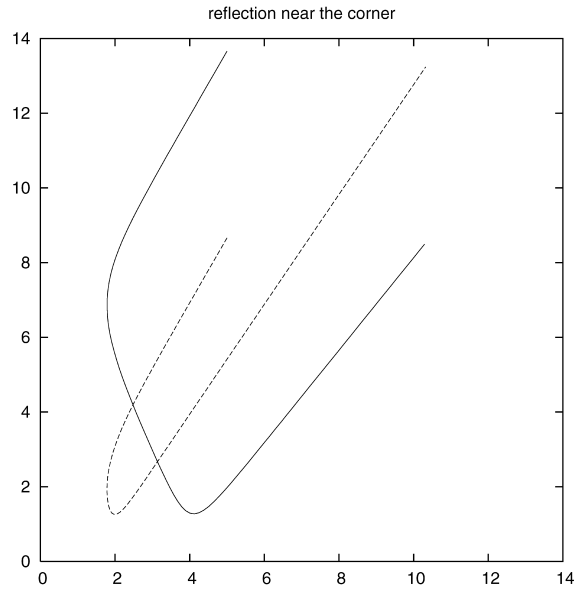

Fig. 15. Motion of the particle near corner.

Before calculating local Lyapunov exponents along the orbit in a rectangular domain, we observe the behavior of exponents when the reflection doesn't happen at all. First of all, we calculate along the solution of the model (1). We set the initial condition $x_0 = y_0 = 10.0$, $v_0 = -\sqrt{0.06}\sin(\pi/6)$, $w_0 = \sqrt{0.06}\cos(\pi/6)$. Let (x, y) be coordinate of the particle and z-axis corresponds to the value of local Lyapunov exponent. The first and second Lyapunov exponents λ_1, λ_2 are shown in Figure 16 and the third and forth λ_3, λ_4 are in 17. Figure at the right of each figure shows projection to the (x, z) plane. In the case of (1), if $\varepsilon < 0$, then the particle converges to asymptotically uniform motion. Thus we can consider that the first and second exponents are always zero corresponding to x, y and the third and forth exponents are always negative corresponding to the velocity (v, w) which converges to a certain constant.

Next, we calculate exponents along the solution of (3) to observe the behavior in the reflection. We set the initial condition $x_0 = y_0 = 10.0$, $v_0 = -\sqrt{0.06}\sin\theta$, $w_0 = \sqrt{0.06}\cos\theta$ so that the particle approaches the wall $x = 0$. Figures 18, 19 and 20 show the exponents corresponding to $\theta = \pi/6, \pi/4, \pi/3$ respectively. Figures upper in each figure shows the first and second exponents and lower shows the third and forth.

In this case, if the particle is away from the wall $x = 0$, then $\lambda_1 = \lambda_2 = 0$ and $\lambda_3, \lambda_4 < 0$ as well as the case of 1. However, when the particle reflects, λ_1

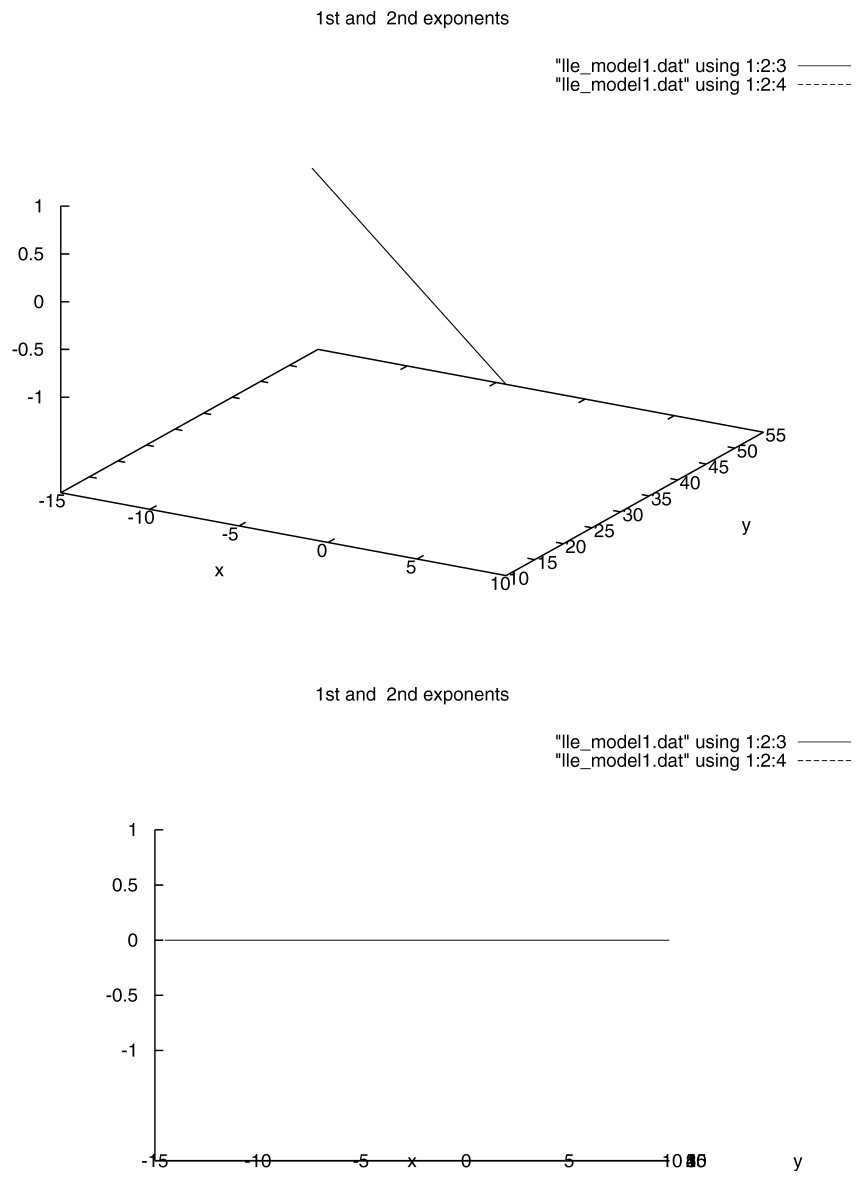

Fig. 16. The first and second local Lyapunov exponents along the solution of (1).

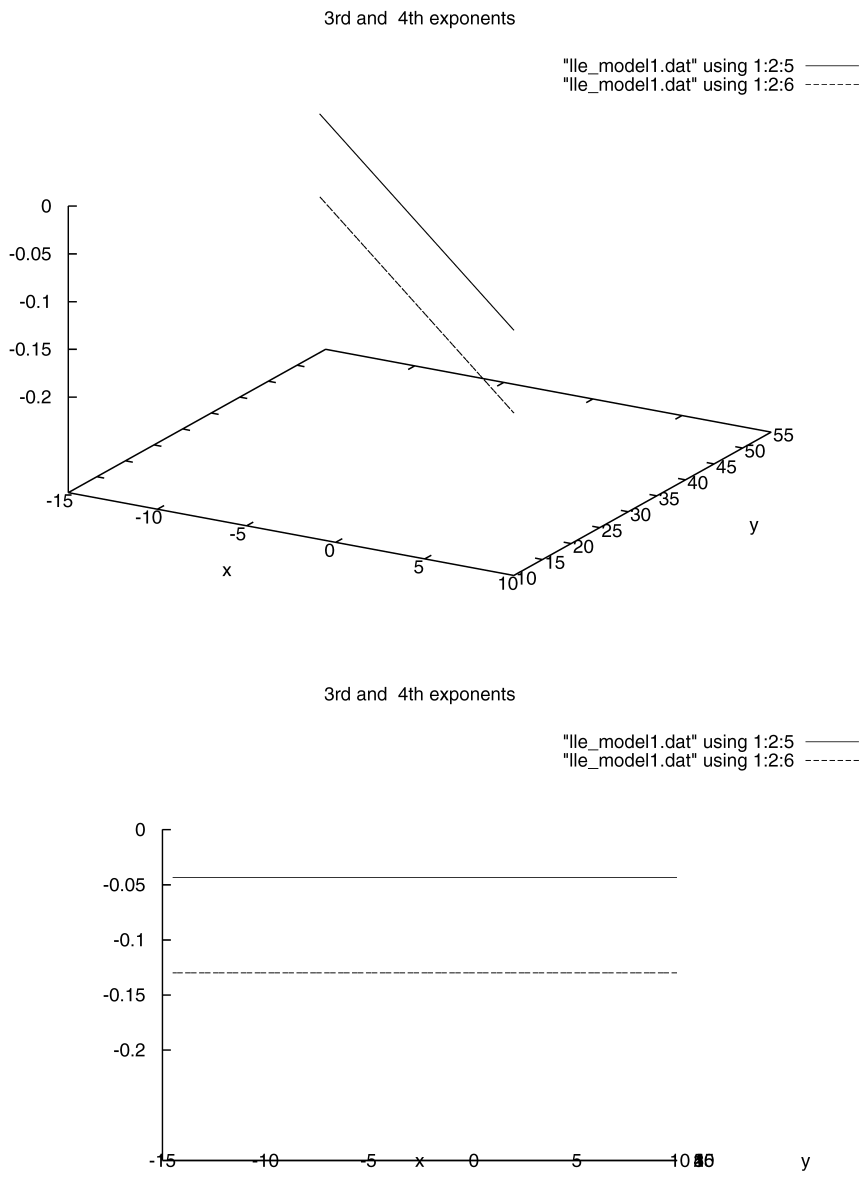

Fig. 17. The third and forth local Lyapunov exponents along the solution of (1).

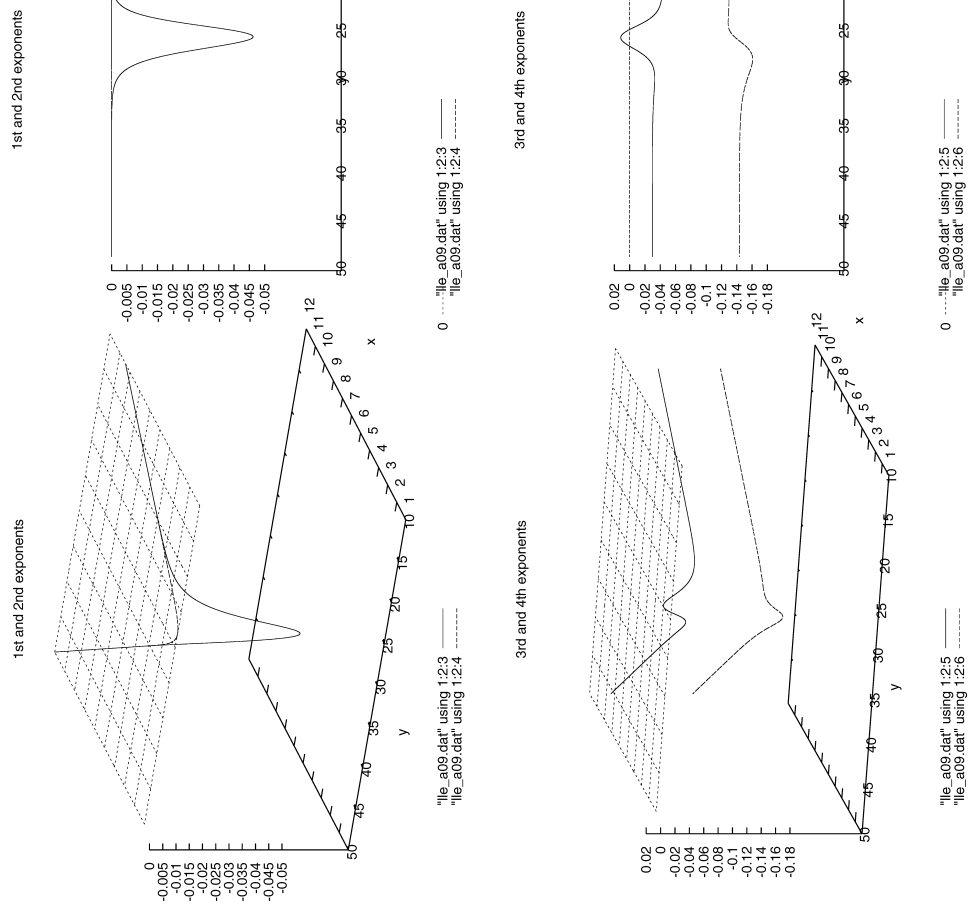

Fig. 18. Local Lyapunov exponents along the orbit of (3) with $\theta = \pi/6$.

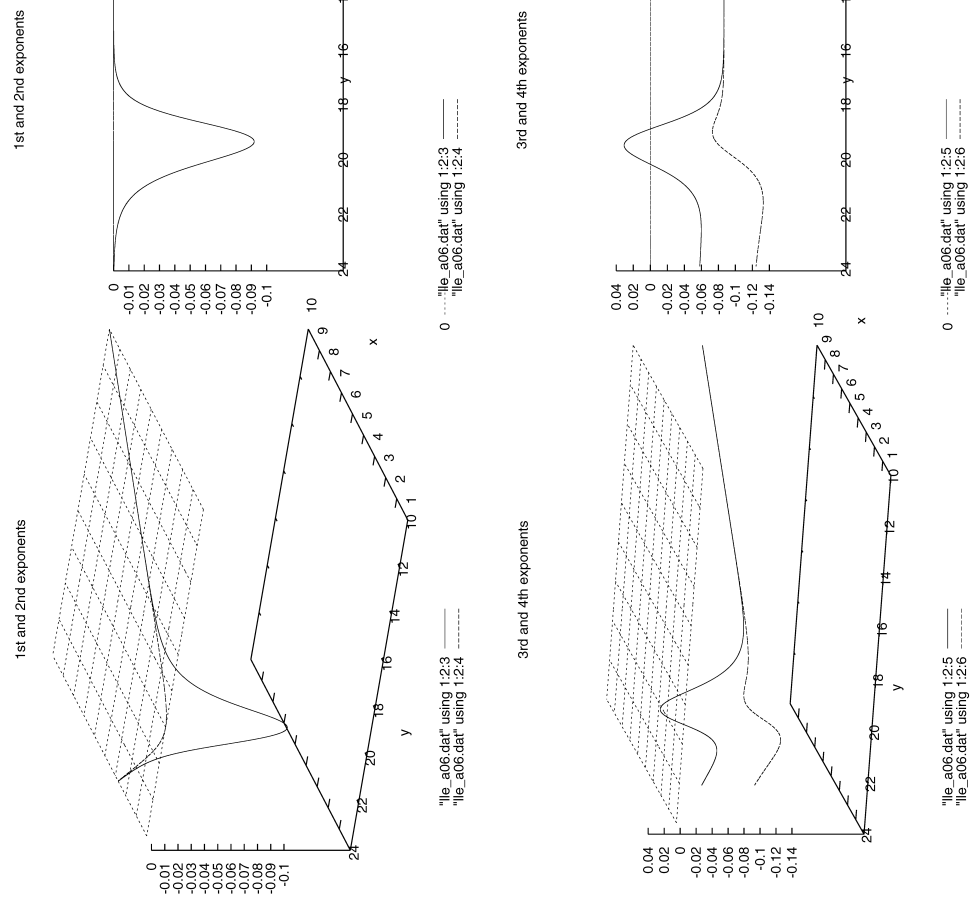

Fig. 19. Local Lyapunov exponents along the orbit of (3) with $\theta = \pi/4$.

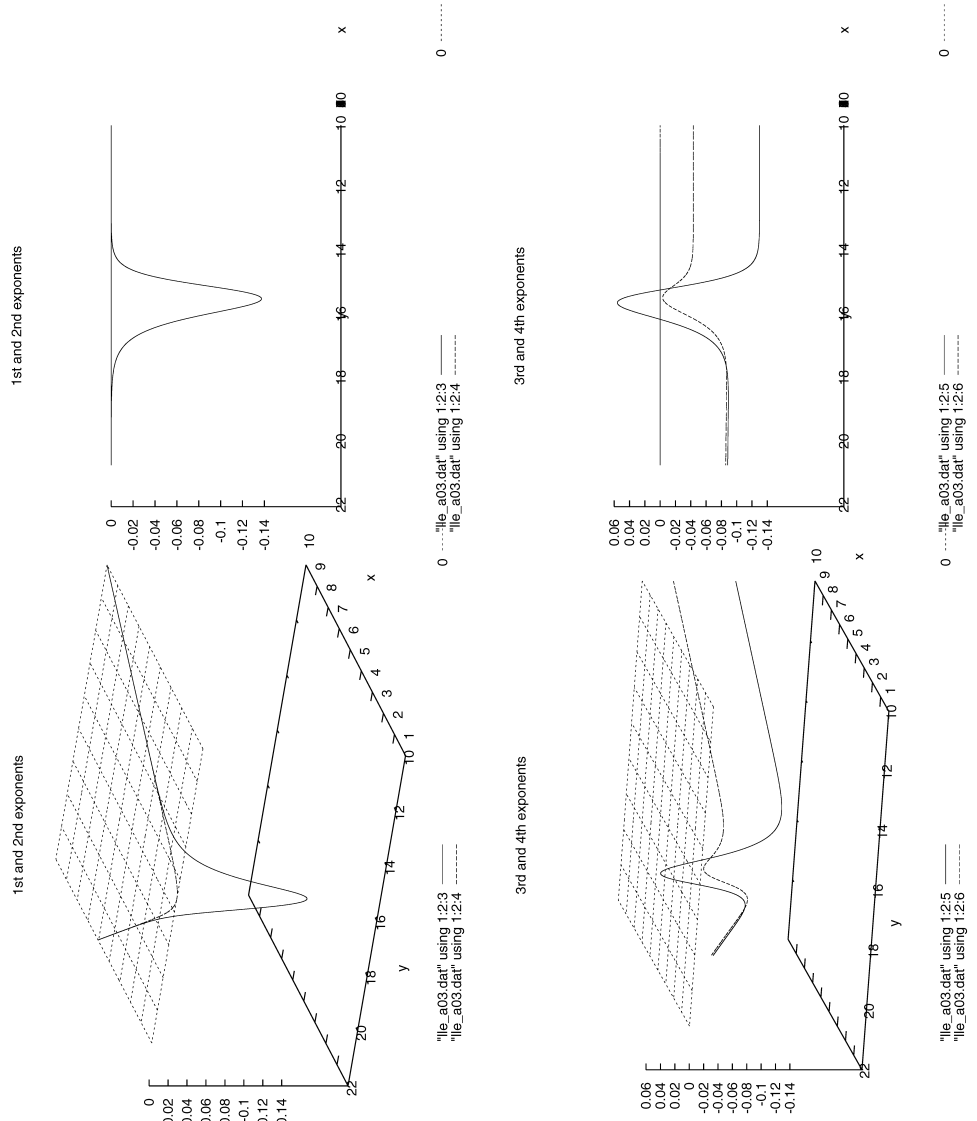

Fig. 20. Local Lyapunov exponents along the orbit of (3) with $\theta = \pi/3$.

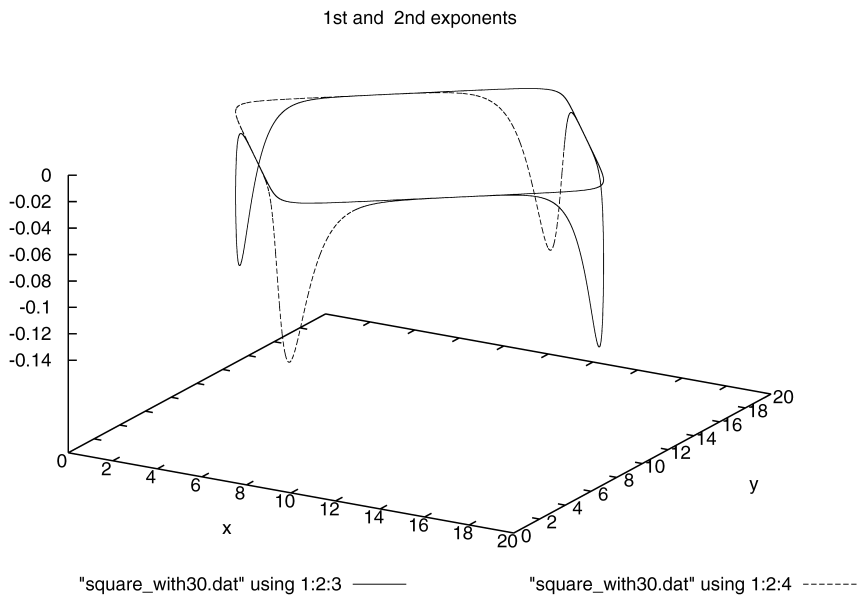

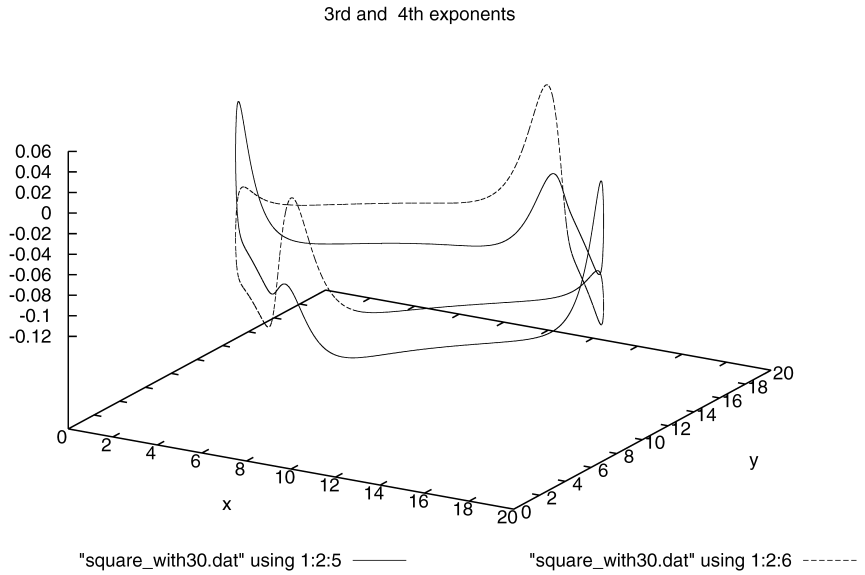

Fig. 21. Local Lyapunov exponents along the stable periodic orbit of 4 with $c = 1.0$ (upper: λ_1, λ_2, lower: λ_1, λ_2).

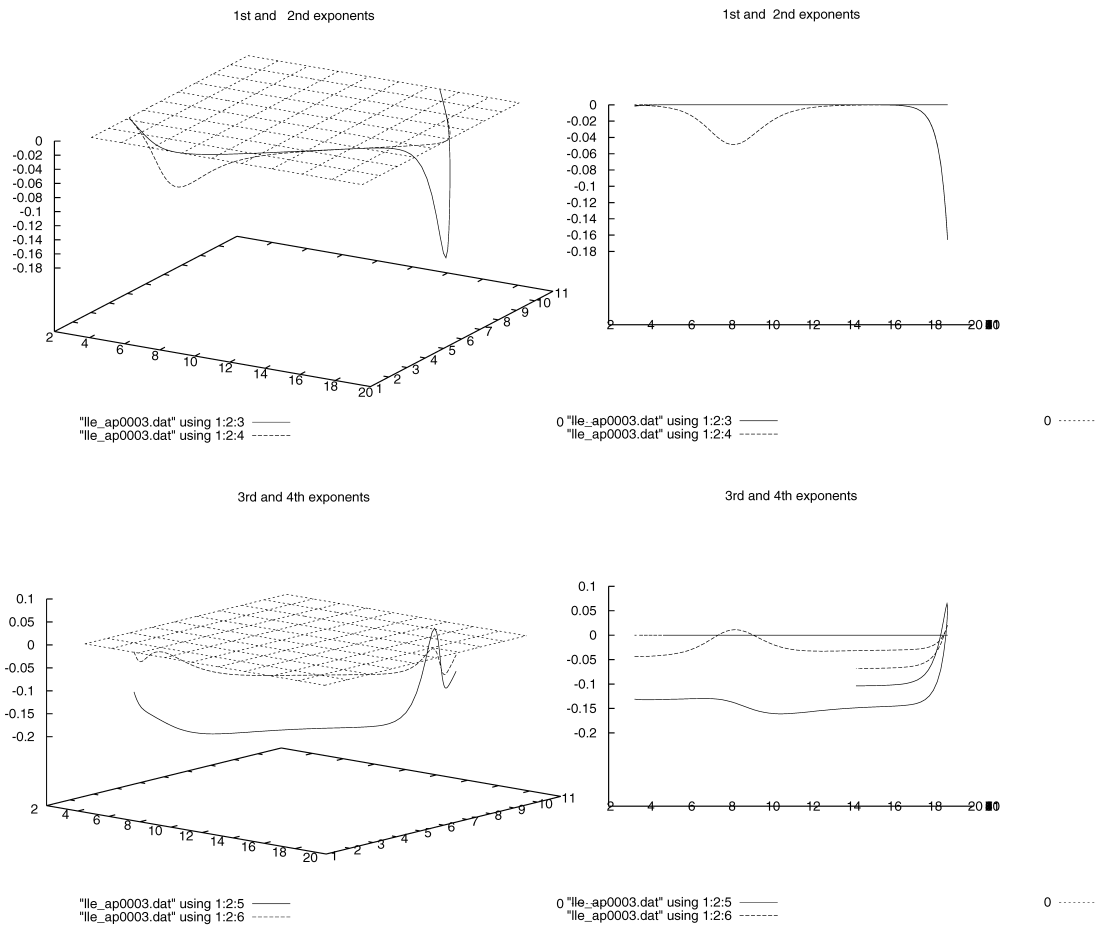

Fig. 22. Local Lyapunov exponents with the angle of incidence $\theta = \pi/6$ and the particle approaching to $(x, y) = (10, 0)$.

becomes negative while λ_2 does not change. On the other hand, when the particle approaches the wall, λ_3 and λ_4 increase temporarily, and λ_3 becomes positive at this time. And when the particle goes away from the wall, λ_3 and λ_4 become negative again.

Then, we observe the behavior along the solution of (4) with $c = 1.0$ in a square domain. Figure 21 shows local Lyapunov exponents along the stable periodic orbit in a square domain. When the particle reflects at $x = 0$ or $x = L$, λ_1 becomes negative and λ_3 becomes positive. Similarly, when the particle reflects at $y = 0$ or $y = L$, λ_2 becomes negative and λ_4 becomes positive. If the particle is away from the wall, exponents behave as well as the case of (1).

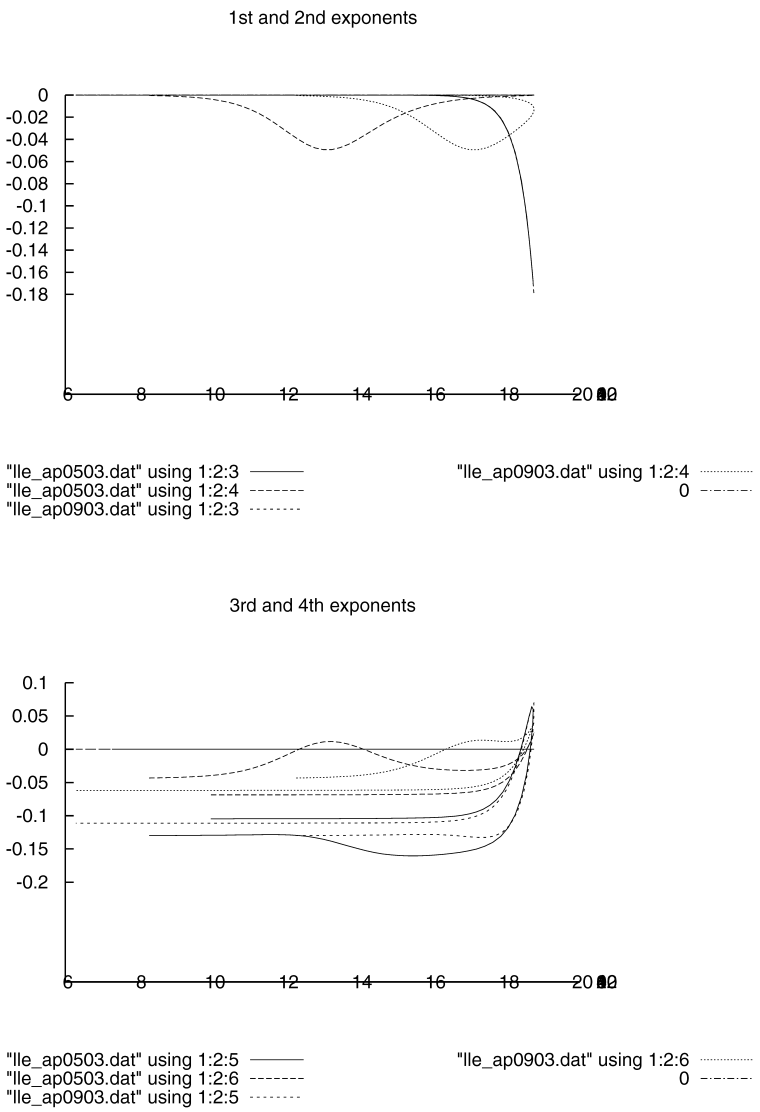

Fig. 23. Local Lyapunov exponents with $\theta = \pi/6$ and the particle approaching to $(x, y) = (15, 0), (19, 0)$ (upper: $\lambda_1,\ \lambda_2,$ lower: $\lambda_3,\ \lambda_4$).

Following the above observation, we consider the reflection at some positions. As it is not essentially related at which wall the particle reflects to the behavior of exponents in a square domain, we think about especially the case where it reflects at $x \leq L/2,\ y = 0$.

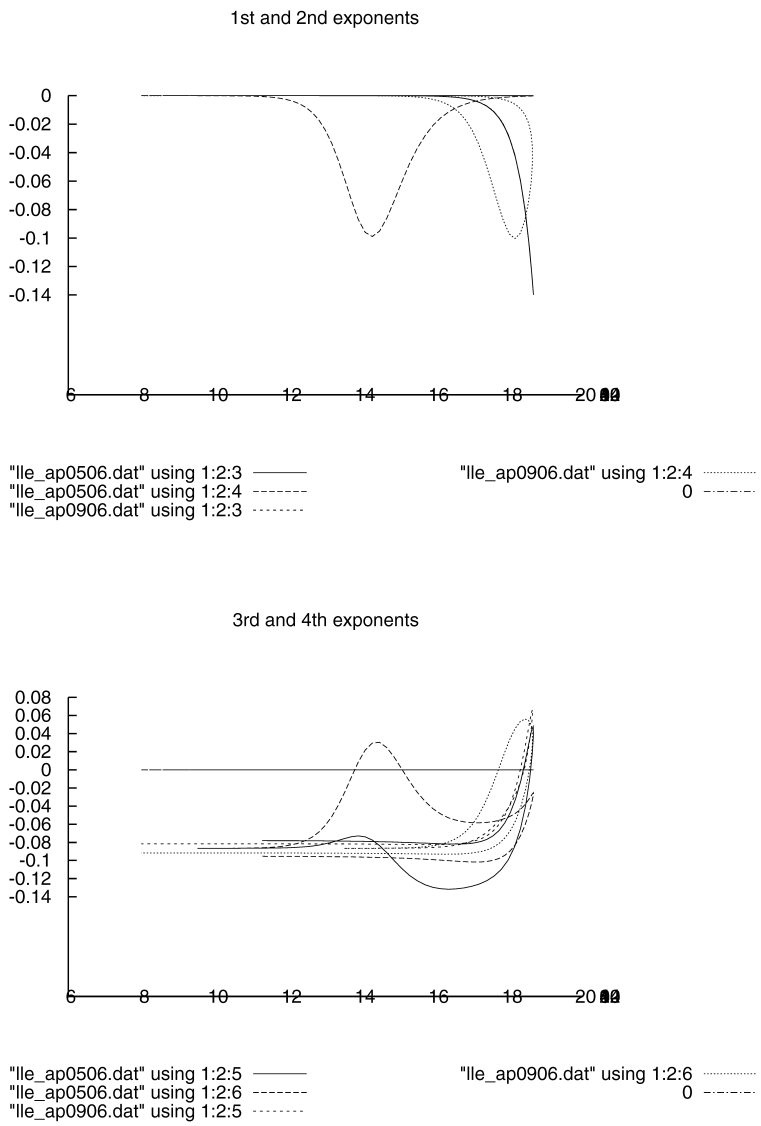

Fig. 24. Local Lyapunov exponents with $\theta = \pi/4$ and the particle approaching to $(x, y) = (15, 0), (19, 0)$ (upper: λ_1, λ_2, lower: λ_3, λ_4).

We assume that $\theta_{\text{in}} = \pi/6$ and the particle approaches the point $(x, y) = (10, 0)$. In this case, exponents behave as well as the case of (3) and then the particle approaches $x = L$. See Figure 22 this might be a natural result, because the reflection position is sufficiently away from other walls.

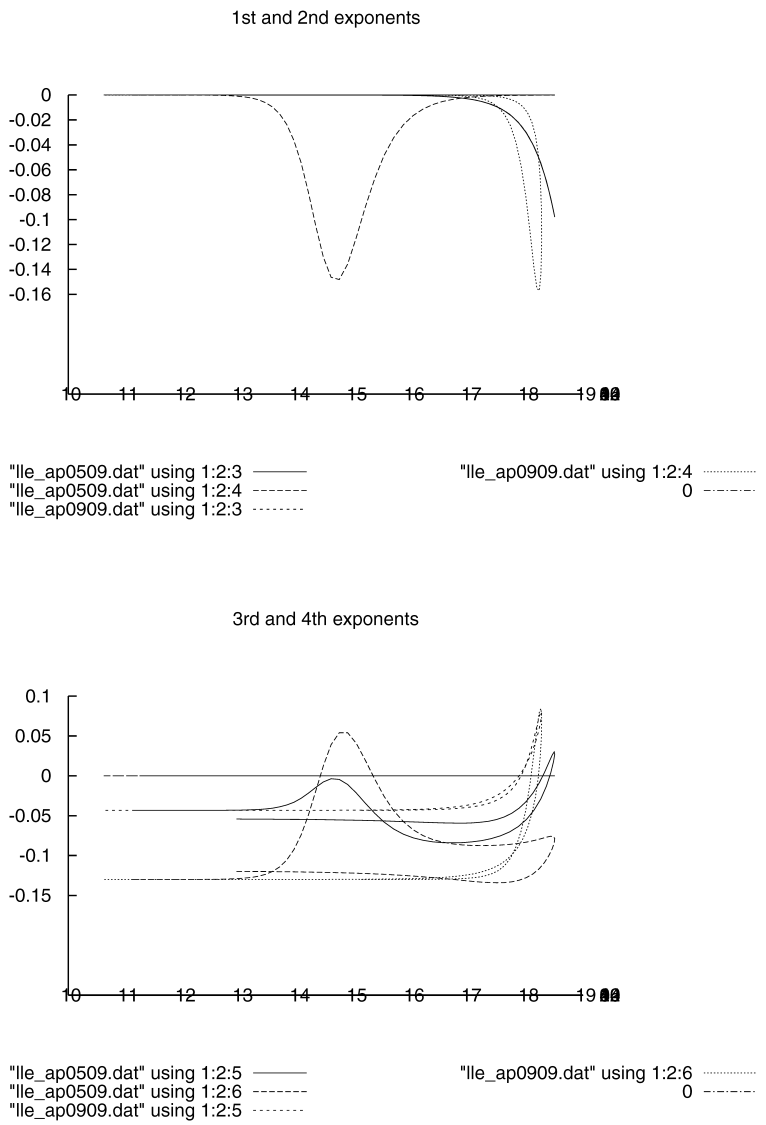

Fig. 25. Local Lyapunov exponents with $\theta = \pi/3$ and the particle approaching to $(15, 0)$, $(19, 0)$ (left: λ_1, λ_2, right: λ_3, λ_4).

Next, we calculate exponents when the particle reflects in the corner of the domain. We assume that $\theta_{\text{in}} = \pi/6$ and the particle approaches the point $(x, y) = (15, 0), (19, 0)$. The result is drawn in (x, z) plane in Figure 23. When the reflection position is near the corner in the domain, before λ_2 that became negative by the reflection returns to zero, λ_1 becomes negative because of

$x = L$. Especially, when the particle approaches $(19, 0)$, λ_1 becomes negative before λ_2 takes a minimal value. And λ_4 increases again without becoming negative after it becomes positive by the reflection. These results mean that the particle already starts reflecting at $x = L$ when reflecting at $y = 0$.

Even if the angle of incidence is changed, similar results are obtained. The reflections with the angle of incidence $\theta = \pi/4$ and $\theta = \pi/3$ are shown in Figure 24 and in Figure 25, respectively.

Thus the effect from another wall grows as the reflection position approaches the corner in the domain. It is thought that the effect from another wall cannot be disregarded when we reduct it to the discrete-time system.

3.3. Modified discrete-time model. From the observation above, we modify the discrete-time model as follows. We suppose that the reflection position divides reflecting wall into $p : 1 - p$. Because the angle of reflection depends on the reflection position, we use p as information of the reflection position. We determine the angle of reflection by

$$\theta_{\text{out}} = G(p, \theta_{\text{in}}) = F(\theta_{\text{in}})g(p). \tag{5}$$

Function $g(p)$ should satisfy the following properties:

(1) The reflection angle is not corrected in the middle point of the wall. $g(1/2) = 1$.

(2) The angle is greatly corrected near the corner in the domain.

Because it is very difficult to derive rigorously the function for the correction, we use the following function with these properties: Let q and r be positive constants.

$$g(p) = \begin{cases} \exp(q(0.5 - p)^r), & \text{if } r \text{ is odd,} \\ \exp(q \operatorname{sign}(0.5 - p)(0.5 - p)^r) & \text{if } r \text{ is even.} \end{cases} \tag{6}$$

The graph of this function and that of (5) are shown in Figure 26.

We simulate the orbit of the particle by using this corrected discrete-time model. However, only periodic orbits appeared though q and r were variously changed. Figure 27 shows the relation between the aspect ratio c of the rectangular domain and reflection positions at $y = 0$.

There seems to be an important property in the motion of the particle that we have overlooked. Then, we observe the reflection for various angle of incidence and modify the discrete-time model more appropriately.

Figure 28 shows the incidence of the particle to a left wall for some angles and initial positions. In the correction above, we assumed that the angle of reflection grew more than usually near the corner in the domain. However, it is not necessarily so. The angle of incidence also effects the correction. That

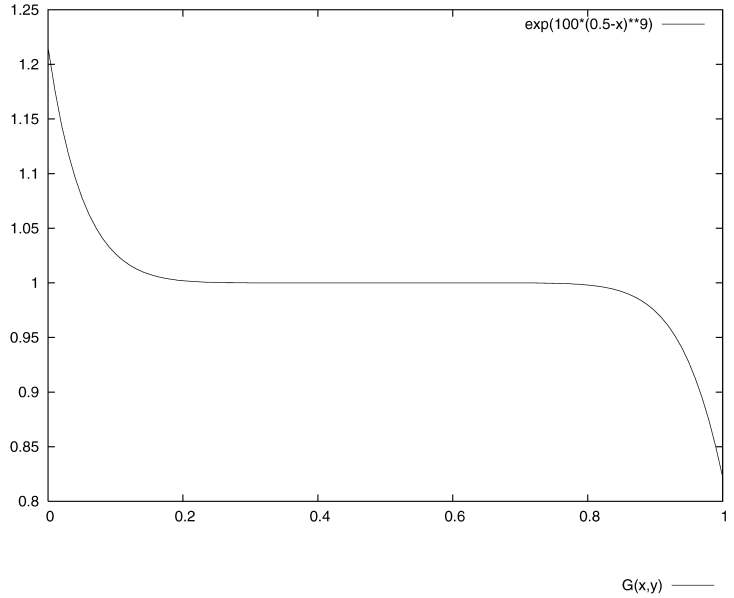

Fig. 26. Function $g(p)$ and corrected function by (5) with $q = 100,\ r = 9$.

is, the angle of reflection becomes smaller for the small angle of incidence and it becomes larger for the large angle of incidence. In consideration of this observation, we use the following function for the correction:

$$g(p, \theta_{\text{in}}) = \exp\left(q\left(\theta_{\text{in}} - \frac{\pi}{4}(0.5 - p)^r \operatorname{sign}(0.5 - p)\right)\right), \tag{7}$$

or

$$g(p, \theta_{\text{in}}) = \exp\left(q\left(\theta_{\text{in}} - \frac{\pi}{4}(0.5 - p)^r\right)\right). \tag{8}$$

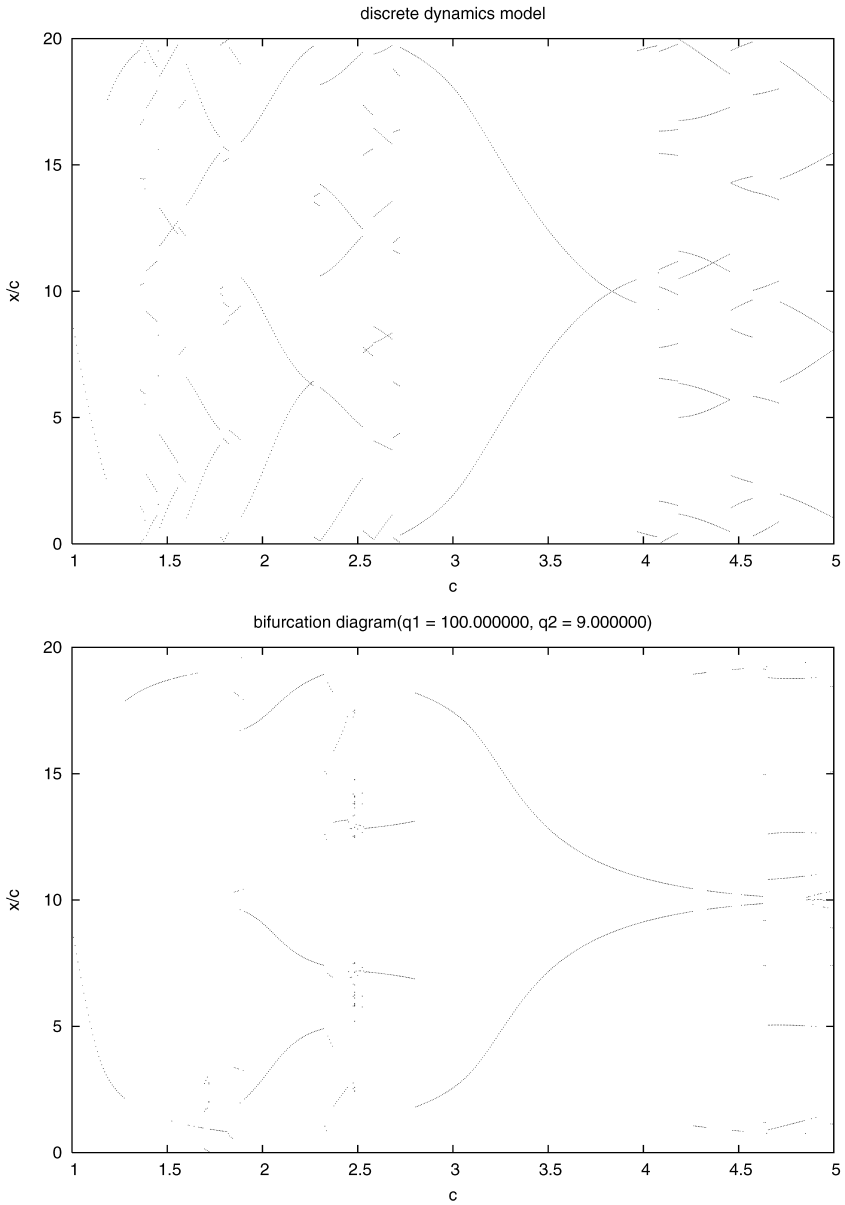

Fig. 27. The relation between the aspect ratio c and reflection positions at $y = 0$ (upper: $q = 7$, $r = 8$, lower: $q = 100$, $r = 9$).

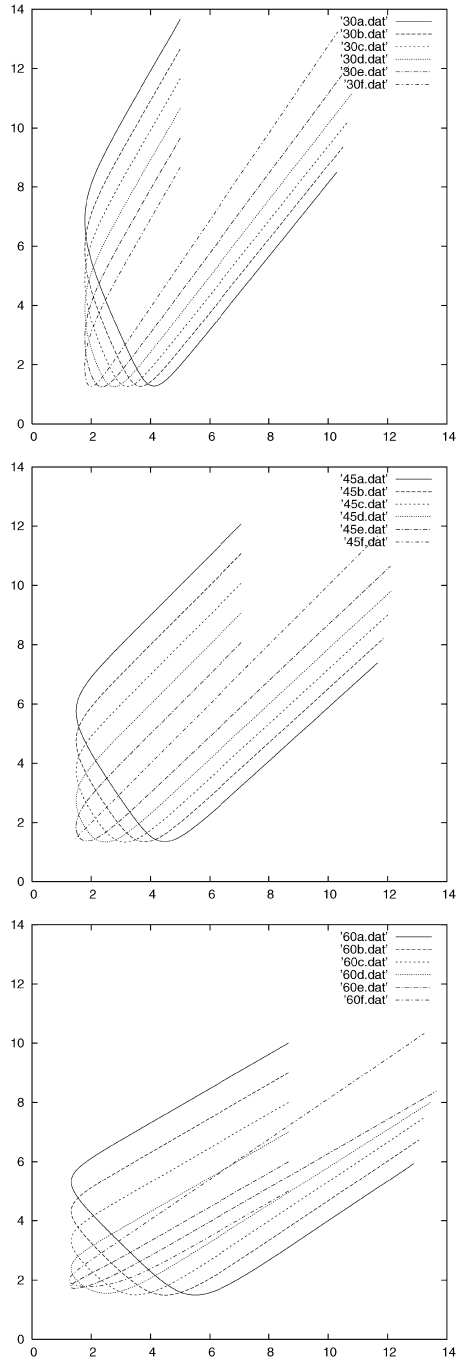

Fig. 28. Reflection near the corner in the domain.

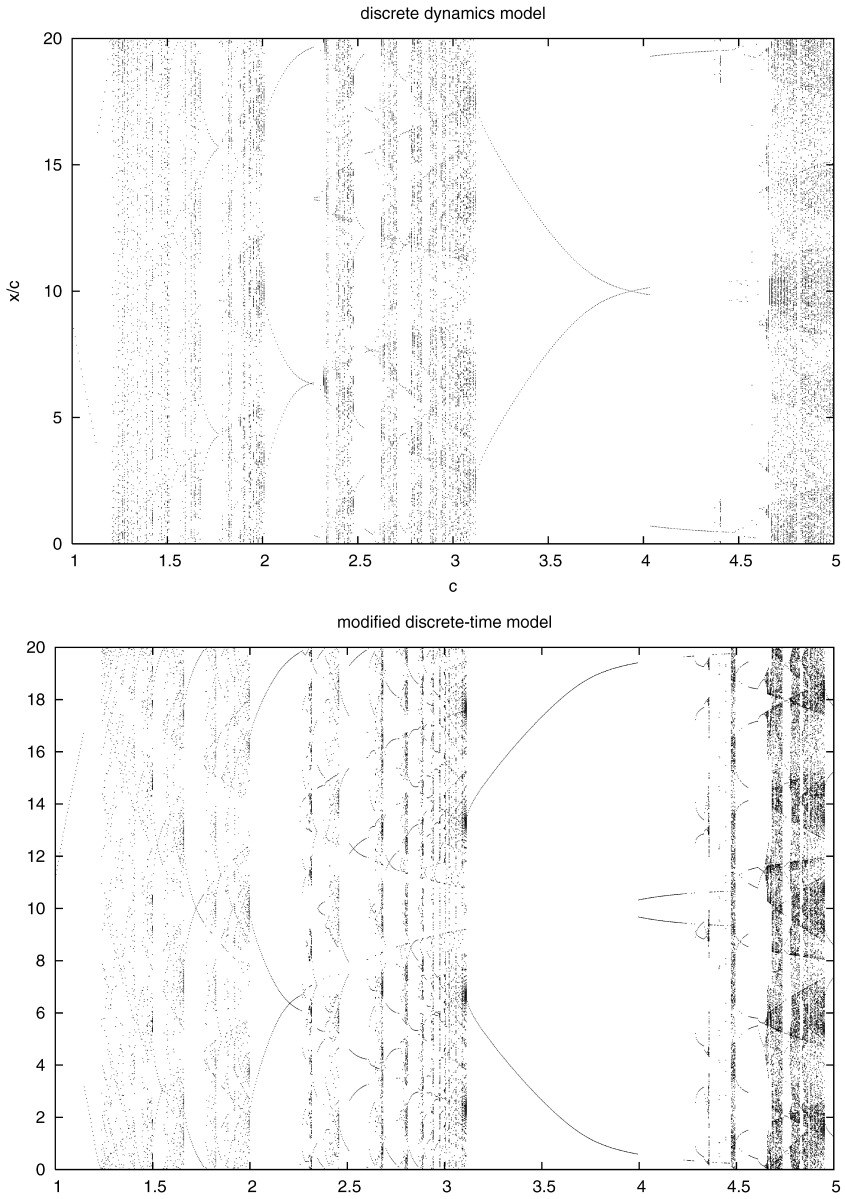

Fig. 29. The relation between the aspect ratio and reflection positions (upper: (7) with $q = 175$, $r = 9$, lower: (8) with $q = 50$, $r = 8$).

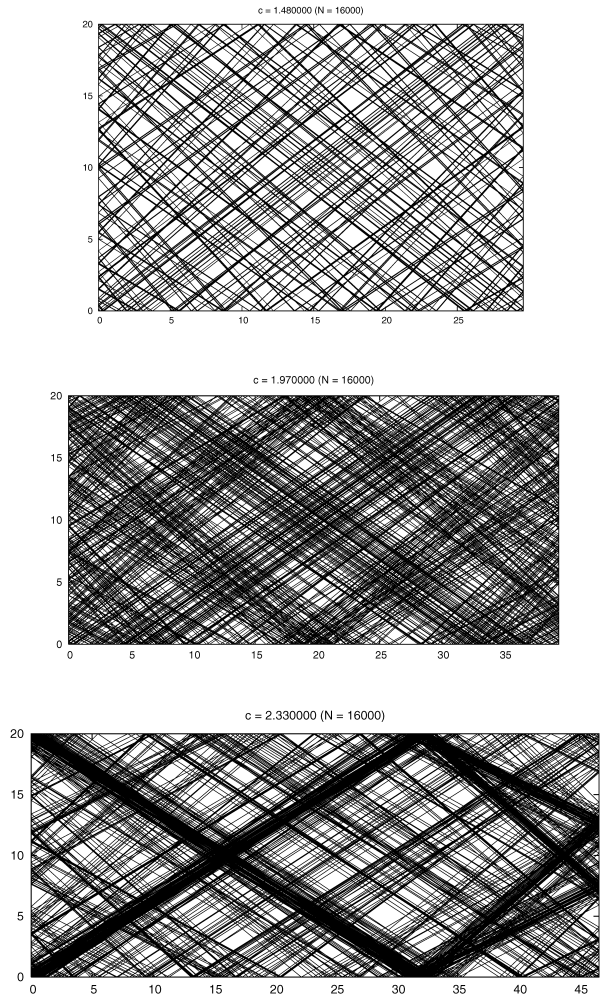

Fig. 30. Non-periodic orbits in the modified discrete-time model.

But it is difficult to derive rigorously the correction function because of the property of the particle model of reflecting without collision.

By use of (7) or (8), we determine the angle of reflection by

$$\theta_{\text{out}} = F(\theta_{\text{in}})g(p, \theta_{\text{in}}). \tag{9}$$

Thus, we can consider the motion of the particle as an essentially two dimensional discrete-time dynamical system defined by the map

$$\begin{pmatrix} \theta_{\text{out}} \\ p \end{pmatrix} \mapsto \begin{pmatrix} G_1(\theta_{\text{out}}, p) \\ G_2(\theta_{\text{out}}, p) \end{pmatrix}. \tag{10}$$

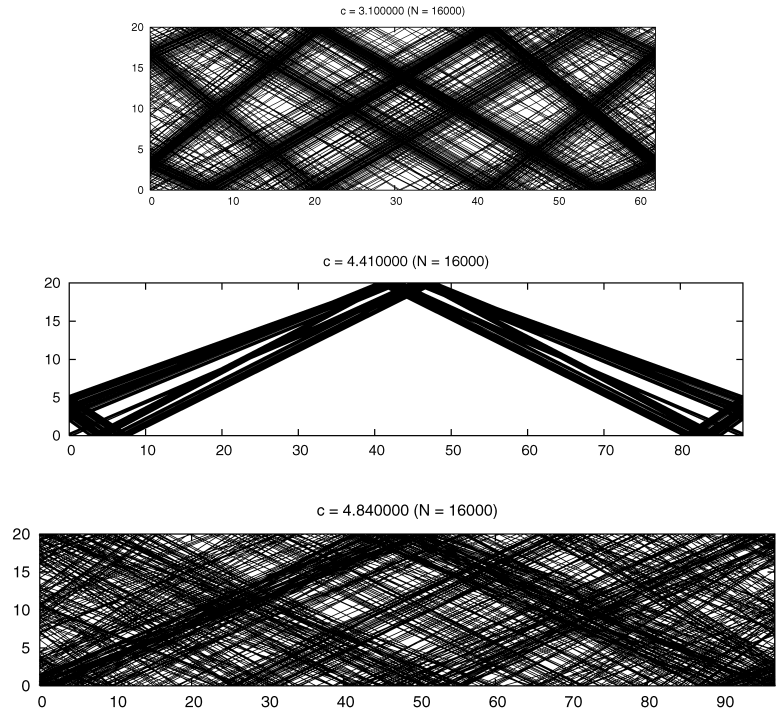

Fig. 30. Continued

Table 2. Lyapunov exponents and dimension for the modified discrete-time model.

Parameter values	Lyapunov spectrum	Lyapunov dimension
$c = 1.00$	$\lambda_1 = -0.3301,$	0.0000
	$\lambda_2 = -0.4502$	
$c = 1.48$	$\lambda_1 = 0.0071,$	1.0103
	$\lambda_2 = -0.6914$	
$c = 1.97$	$\lambda_1 = 0.0431,$	1.0592
	$\lambda_2 = -0.7276$	
$c = 2.33$	$\lambda_1 = 0.1444,$	1.1977
	$\lambda_2 = -0.7303$	
$c = 2.91$	$\lambda_1 = -0.0050,$	0.0000
	$\lambda_2 = -0.6302$	
$c = 3.10$	$\lambda_1 = 0.0521,$	1.0756
	$\lambda_2 = -0.6900$	
$c = 3.12$	$\lambda_1 = -0.1583,$	0.0000
	$\lambda_2 = -0.6372$	
$c = 4.41$	$\lambda_1 = 0.0704,$	1.1309
	$\lambda_2 = -0.5381$	
$c = 4.84$	$\lambda_1 = 0.2170,$	1.3080
	$\lambda_2 = -0.7046$	

We simulate the orbit in a rectangular domain by using this formula. Figure 29 shows the relation between the aspect ratio c of the rectangular domain and reflection positions at $y = 0$. This modified discrete-time system shows the fault structure of periodic orbits and non-periodic orbits.

Non-periodic orbits in the discrete-time model are similar to those in the particle model. Compare Figure 30 and 9. Then, we calculate Lyapunov exponents for these non-periodic orbits. We consider the modified discrete-time system as two dimensional system. So we pay attention to the sign of two exponents. Table 2 shows Lyapunov exponents obtained by using the correction function (7) with $q = 175$, $r = 9$. The result is almost the same as that in the case of the particle model. For a simple periodic orbit appearing

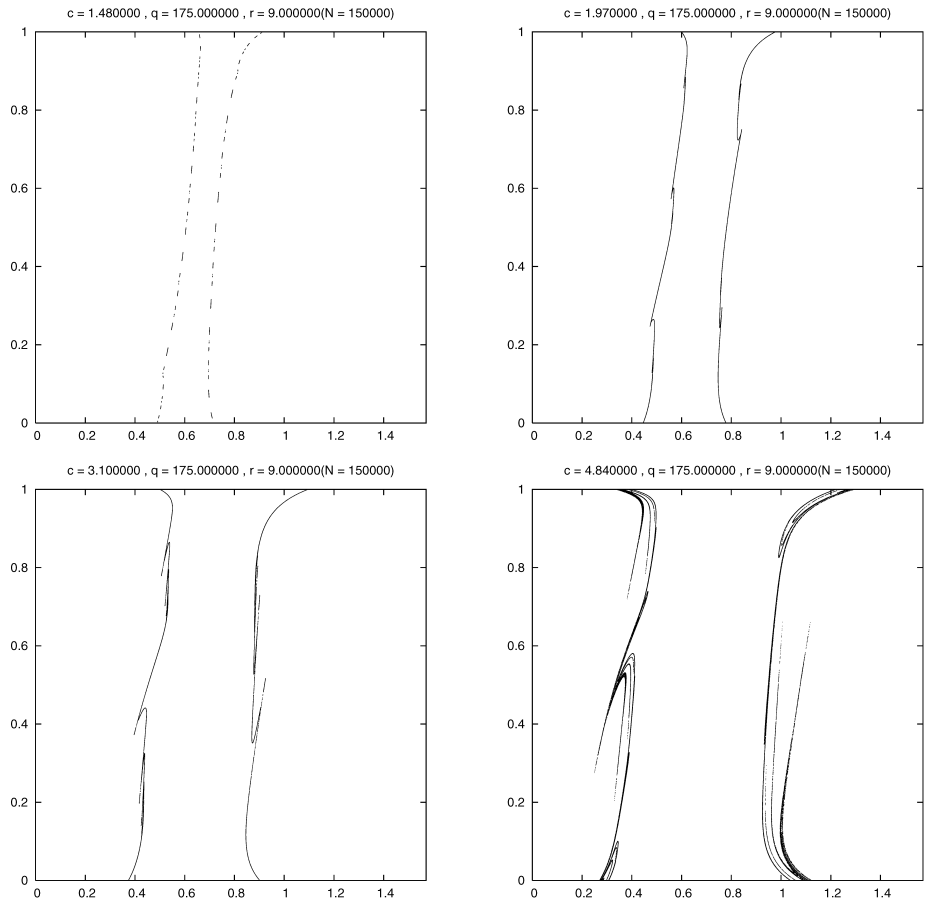

Fig. 31. Orbits defined by the modified discrete-time model plotted on (θ_{in}, p)-plane.

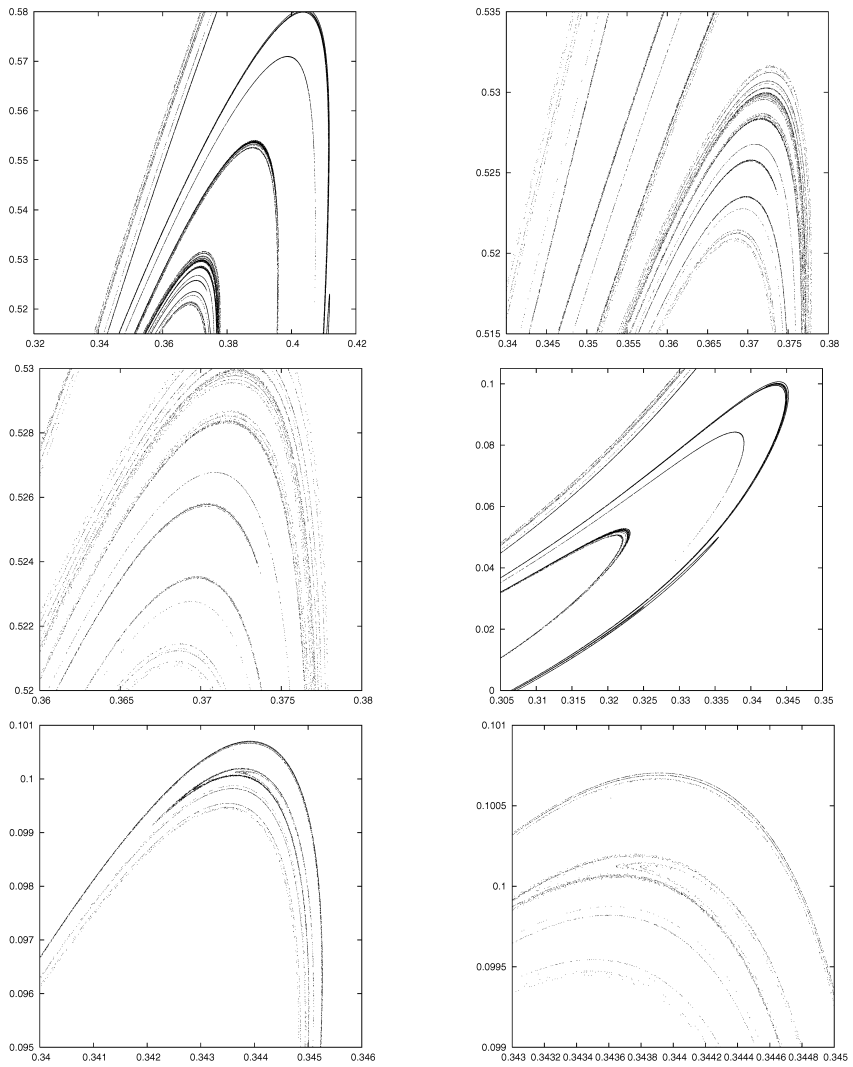

Fig. 32. Strange structure observed in the orbit for $c = 4.84$.

near $c = 1.0$, the sign of exponents become $(-, -)$ and the Lyapunov dimension $d_{\mathrm{L}} = 0.0$. These are the same for other periodic orbits. On the other hand, a positive exponent appears for non-periodic orbit. In this case, the sign of two exponents is $(+, -)$ and d_{L} becomes a fractal dimension $1 < d_{\mathrm{L}} < 2$. Even if parameters of the correction function q, r are changed, a similar result is obtained.

Non-periodic orbits in the modified discrete-time model have an interesting feature. Plot sequence of points (θ_{in}, p) defined by the map (10) on the plane after a sufficient long calculation. Naturally, when a periodic orbit appears in a rectangular domain, the attractor becomes a periodic point. On the other hand, the more complex structure appears for the orbit with a positive Lyapunov exponent as shown in Figure 31. Furthermore, the nest structure like the fractal can be observed by expanding a part the orbit for $c = 4.84$ as shown in Figure 32.

In the final part of this paper, we again emphasize that the strange behavior of the solutions of the system is due to the existence of an intermittent-type chaotic attractor, and we elucidate it numerically at the first time for this interesting problem. Surprisingly, this is simply because the reflection rule at the corner is irregular a little. We are a little interested in the fact that such a small effect raises the serious result in this nonlinear and non-equilibrium system. We expect in the future that our result is improved and is made precise more and more especially in mathematically rigorous point of view.

References

[1] S.-I. Ei, M. Mimura and M. Nagayama, Interacting spots in reaction diffusion systems, DCDS, **14** (2006), 31–62.

[2] J. D. Farmer, E. Ott and J. A. Yorke, The dimension of chaotic attractors, Physica, **7D** (1983), 153–180.

[3] Y. Hayashima, M. Nagayama and S. Nakata, A camphor oscillates while breaking symmetry, J. Phys. Chem. B, **105** (2001), 5353–5357.

[4] T. Matsumoto, "A billiard problem under nonlinear and nonequilibrium condition (in Japanese)", Master Thesis in Hiroshima University, (2002).

[5] M. Matsumoto, "Analysis of the particle model by which camphor movement is described (in Japanese)", Master Thesis in Hiroshima University, (2001).

[6] T. Morihara, "A nonequilibrium billiard problem (in Japanese)", Master Thesis in Hiroshima University, (2003).

[7] I. Shimada, and T. Nagashima, A numerical approach to ergodic problem of dissipative dynamical systems, Progr. Theoret. Phys., **61** (1979), 1605–1616.

[8] A. Wolf, J. B. Swift, H. L. Swinney and J. A. Vastano, Determining Lyapunov exponents from a time series, Physica, **16D** (1985), 285–317.

Masayasu Mimura
Department of Mathematics
School of Science and Technology
Meiji University
Kawasaki 214-8571 *Japan*
E-mail: mimura@math.meiji.ac.jp

Tomoyuki Miyaji
Department of Mathematical and Life Sciences
Graduate School of Science
Hiroshima University
Higashi-Hiroshima 739-8526 *Japan*
E-mail: denpaatama@hiroshima-u.ac.jp

Isamu Ohnishi
Department of Mathematical and Life Sciences
Graduate School of Science
Hiroshima University
Higashi-Hiroshima 739-8526 *Japan*
E-mail: isamu_o@math.sci.hiroshima-u.ac.jp